04.sup Equations of Motion and Applied Fields*

Prof. Steven M. Lund
Physics and Astronomy Department
Facility for Rare Isotope Beams (FRIB)
Michigan State University (MSU)

PHY 905 Lectures
"Accelerator Physics"
Steven M. Lund and Yue Hao

Michigan State University, Spring Semester 2018
(Version 20180130)

* Research supported by:
FRIB/MSU: U.S. Department of Energy Office of Science Cooperative Agreement DE-SC0000661and National Science Foundation Grant No. PHY-1102511

S1: Particle Equations of Motion
S1A: Introduction: The Lorentz Force Equation

The *Lorentz force equation* of a charged particle is given by (MKS Units):

$$\frac{d}{dt}\mathbf{p}_i(t) = q_i\left[\mathbf{E}(\mathbf{x}_i,t) + \mathbf{v}_i(t)\times\mathbf{B}(\mathbf{x}_i,t)\right]$$

$m_i,\ q_i$ .... particle mass, charge — i = particle index

$\mathbf{x}_i(t)$ .... particle coordinate — t = time

$\mathbf{p}_i(t) = m_i\gamma_i(t)\mathbf{v}_i(t)$ .... particle momentum

$\mathbf{v}_i(t) = \frac{d}{dt}\mathbf{x}_i(t) = c\vec{\beta}_i(t)$ .... particle velocity

$\gamma_i(t) = \frac{1}{\sqrt{1-\beta_i^2(t)}}$ .... particle gamma factor

	Total		Applied		Self
Electric Field:	$\mathbf{E}(\mathbf{x},t)$	$=$	$\mathbf{E}^a(\mathbf{x},t)$	$+$	$\mathbf{E}^s(\mathbf{x},t)$
Magnetic Field:	$\mathbf{B}(\mathbf{x},t)$	$=$	$\mathbf{B}^a(\mathbf{x},t)$	$+$	$\mathbf{B}^s(\mathbf{x},t)$

S1B: Applied Fields used to Focus, Bend, and Accelerate Beam

Transverse optics for focusing:

Electric Quadrupole

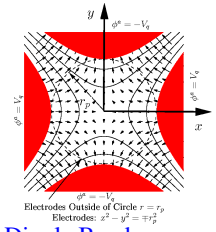

Magnetic Quadrupole

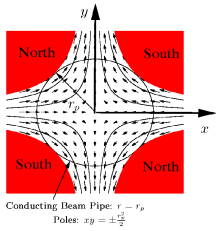

Solenoid

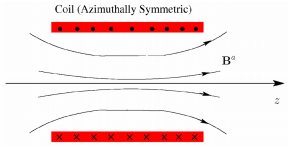

Dipole Bends:

Electric *x*-direction bend

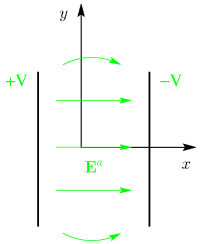

Magnetic *x*-direction bend

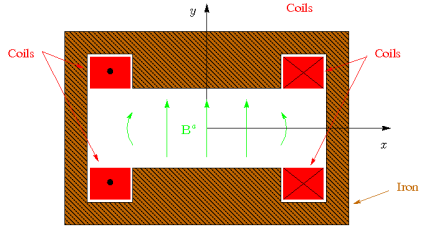

Longitudinal Acceleration:

RF Cavity

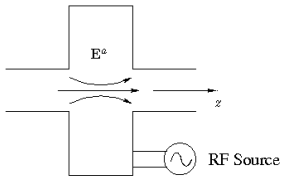

Induction Cell

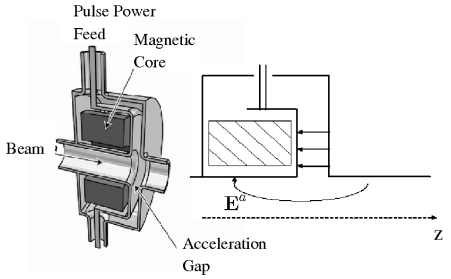

We will cover primarily transverse dynamics. Lectures by J.J. Barnard will cover acceleration and longitudinal physics:

- Acceleration influences transverse dynamics – not possible to fully decouple

S1C: Machine Lattice

Applied field structures are often arraigned in a regular (periodic) lattice for beam transport/acceleration:

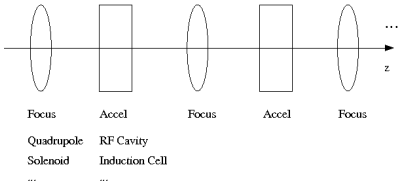

- Sometimes functions like bending/focusing are combined into a single element

Example – Linear FODO lattice (symmetric quadrupole doublet)

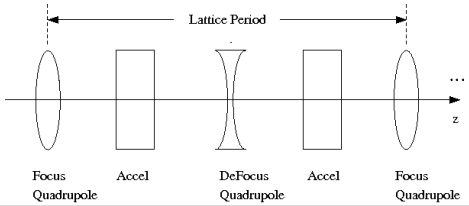

Lattices for rings and some beam insertion/extraction sections also incorporate bends and more complicated periodic structures:

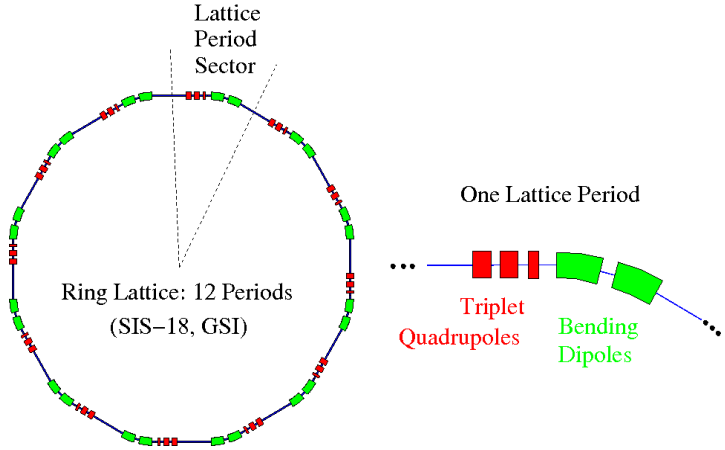

- Elements to insert beam into and out of ring further complicate lattice
- Acceleration cells also present
  (typically several RF cavities at one or more location)

S1D: Self fields

Self-fields are generated by the distribution of beam particles:
Charges
Currents

Particle at Rest
(pure electrostatic)

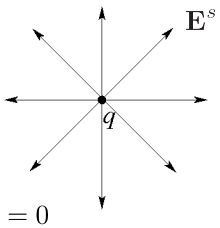

$\mathbf{B}^s = 0$

Particle in Motion

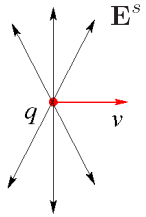

Obtain from Lorentz boost of rest-frame field: see Jackson, *Classical Electrodynamics*

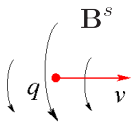

- Superimpose for all particles in the beam distribution
- Accelerating particles also radiate
  - We neglect electromagnetic radiation in this class
    (see: J.J. Barnard, Intro Lectures)

The electric ($\mathbf{E}^a$) and magnetic ($\mathbf{B}^a$) fields satisfy the Maxwell Equations. The linear structure of the Maxwell equations can be exploited to resolve the field into Applied and Self-Field components:

$$\mathbf{E} = \mathbf{E}^a + \mathbf{E}^s$$

$$\mathbf{B} = \mathbf{B}^a + \mathbf{B}^s$$

Applied Fields (often quasi-static $\partial/\partial t \simeq 0$) $\mathbf{E}^a$, $\mathbf{B}^a$
Generated by elements in lattice

$$\nabla \cdot \mathbf{E}^a = \frac{\rho^a}{\epsilon_0} \qquad \nabla \times \mathbf{B}^a = \mu_0 \mathbf{J}^a + \frac{1}{c^2}\frac{\partial}{\partial t}\mathbf{E}^a$$

$$\nabla \times \mathbf{E}^a = -\frac{\partial}{\partial t}\mathbf{B}^a \qquad \nabla \cdot \mathbf{B}^a = 0$$

ρ^a = applied charge density
$\mathbf{J}^a$ = applied current density

$$\frac{1}{\mu_0 \epsilon_0} = c^2$$

+ Boundary Conditions on $\mathbf{E}^a$ and $\mathbf{B}^a$

- Boundary conditions depend on the total fields $\mathbf{E}$, $\mathbf{B}$
  and if separated into Applied and Self-Field components, care can be required
- System often solved as static boundary value problem and source free in the vacuum transport region of the beam

/// Aside: Notation:

$$\nabla \equiv \hat{\mathbf{x}}\frac{\partial}{\partial x} + \hat{\mathbf{y}}\frac{\partial}{\partial y} + \hat{\mathbf{z}}\frac{\partial}{\partial z}$$ - Cartesian Representation

$$= \hat{\mathbf{r}}\frac{\partial}{\partial r} + \frac{\hat{\theta}}{r}\frac{\partial}{\partial \theta} + \hat{\mathbf{z}}\frac{\partial}{\partial z}$$ - Cylindrical Representation

$x = r\cos\theta \qquad \hat{\mathbf{r}} = \hat{\mathbf{x}}\cos\theta + \hat{\mathbf{y}}\sin\theta$

$y = r\sin\theta \qquad \hat{\theta} = -\hat{\mathbf{x}}\sin\theta + \hat{\mathbf{y}}\cos\theta$

$$= \frac{\partial}{\partial \mathbf{x}}$$ - Abbreviated Representation

$$= \frac{\partial}{\partial \mathbf{x}_\perp} + \hat{\mathbf{z}}\frac{\partial}{\partial z}$$ - Resolved Abbreviated Representation

Resolved into Perpendicular $(\perp)$ and Parallel (z) components

$\mathbf{x} = \hat{\mathbf{x}}x + \hat{\mathbf{y}}y + \hat{\mathbf{z}}z$

$= \mathbf{x}_\perp + \hat{\mathbf{z}}z \qquad \mathbf{x}_\perp \equiv \hat{\mathbf{x}}x + \hat{\mathbf{y}}y$

In integrals, we denote:

$$\int d^3x \cdots = \int_{-\infty}^{\infty} dx \int_{-\infty}^{\infty} dy \int_{-\infty}^{\infty} dz \cdots = \int d^2x_\perp \int_{-\infty}^{\infty} dz \cdots$$

$$\int d^2x_\perp \cdots = \int_{-\infty}^{\infty} dx \int_{-\infty}^{\infty} dy \cdots = \int_0^{\infty} dr\, r \int_{-\pi}^{\pi} d\theta \cdots$$

///

Self-Fields (dynamic, evolve with beam)

Generated by particle of the beam rather than (applied) sources outside beam

$$\nabla \cdot \mathbf{E}^s = \frac{\rho^s}{\epsilon_0} \qquad \nabla \times \mathbf{B}^s = \mu_0 \mathbf{J}^s + \frac{1}{c^2}\frac{\partial}{\partial t}\mathbf{E}^s$$

$$\nabla \times \mathbf{E}^s = -\frac{\partial}{\partial t}\mathbf{B}^s \qquad \nabla \cdot \mathbf{B}^s = 0$$

i = particle index (N particles)

ρ^s = beam charge density $= \sum_{i=1}^{N} q_i \delta[\mathbf{x} - \mathbf{x}_i(t)]$

q_i = particle charge

$\mathbf{x}_i$ = particle coordinate

$\mathbf{v}_i$ = particle velocity

$\mathbf{J}^s$ = beam current density $= \sum_{i=1}^{N} q_i \mathbf{v}_i(t) \delta[\mathbf{x} - \mathbf{x}_i(t)]$

$\delta(\mathbf{x}) \equiv \delta(x)\delta(y)\delta(z)$

$\delta(x) \equiv$ Dirac-delta function

$\sum_{i=1}^{N} \cdots =$ sum over beam particles

+ Boundary Conditions on $\mathbf{E}^s$ and $\mathbf{B}^s$ from material structures, radiation conditions, etc.

In accelerators, typically there is ideally a single species of particle:

$q_i \to q$

$m_i \to m$

Large Simplification!

Multi-species results in more complex collective effects

Motion of particles within axial slices of the "bunch" are highly directed:

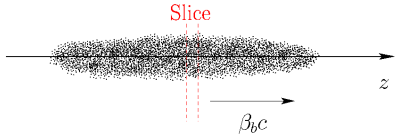

$$\beta_b(z)c \equiv \frac{1}{N'}\sum_{i=1}^{N'} \mathbf{v}_i \cdot \hat{\mathbf{z}}$$

$=$ Mean axial velocity of N' particles in beam slice

$$\frac{d}{dt}\mathbf{x}_i(t) = \mathbf{v}_i(t) = \hat{\mathbf{z}}\beta_b(z)c + \delta\mathbf{v}_i$$

$|\delta \mathbf{v}_i| \ll |\beta_b| c$ Paraxial Approximation

There are typically many particles: (see S13, Vlasov Models for more details)

$$\rho^s = \sum_{i=1}^{N} q_i \delta[\mathbf{x} - \mathbf{x}_i(t)] \simeq \rho(\mathbf{x}, t)$$ continuous charge-density

$$\mathbf{J}^s = \sum_{i=1}^{N} q_i \mathbf{v}_i(t) \delta[\mathbf{x} - \mathbf{x}_i(t)] \simeq \beta_b c \rho(\mathbf{x}, t)\hat{\mathbf{z}}$$ continuous axial current-density

The beam evolution is typically sufficiently slow (for heavy ions) where we can neglect radiation and approximate the self-field Maxwell Equations as:

See: Appendix B, Magnetic Self-Fields and

J. J. Barnard, Intro. Lectures: Electrostatic Approximation

$$\mathbf{E}^s = -\nabla\phi$$

$$\mathbf{B}^s = \nabla \times \mathbf{A} \qquad \mathbf{A} = \hat{\mathbf{z}}\frac{\beta_b}{c}\phi$$

$$\nabla^2\phi = \frac{\partial}{\partial \mathbf{x}} \cdot \frac{\partial}{\partial \mathbf{x}}\phi = -\frac{\rho^s}{\epsilon_0}$$

+ Boundary Conditions on ϕ

Vast Reduction of self-field model:

Approximation equiv to electrostatic interactions in frame moving with beam: see Appendix B

But still complicated

Resolve the Lorentz force acting on beam particles into Applied and Self-Field terms:

$$\mathbf{F}_i(\mathbf{x}_i, t) = q\mathbf{E}(\mathbf{x}_i, t) + q\mathbf{v}_i(t) \times \mathbf{B}(\mathbf{x}_i, t)$$

$\mathbf{F}_i = \mathbf{F}_i^a + \mathbf{F}_i^s$

$\mathbf{E} = \mathbf{E}^a + \mathbf{E}^s$

$\mathbf{B} = \mathbf{B}^a + \mathbf{B}^s$

Applied:

$$\mathbf{F}_i^a = q\mathbf{E}_i^a + q\mathbf{v}_i \times \mathbf{B}_i^a$$

$\mathbf{E}^a(\mathbf{x}_i, t) \equiv \mathbf{E}_i^a$ etc.

Self-Field:

$$\mathbf{F}_i^s = q\mathbf{E}_i^s + q\mathbf{v}_i \times \mathbf{B}_i^s$$

The self-field force can be simplified:

- See also: J.J. Barnard, Intro. Lectures

Plug in self-field forms:

$$\mathbf{F}_i^s = q\mathbf{E}_i^s + q\mathbf{v}_i \times \mathbf{B}_i^s \qquad \sim 0 \quad \text{Neglect: Paraxial} \qquad \cdots\Big|_i \equiv \cdots\Big|_{\mathbf{x}=\mathbf{x}_i}$$

$$\simeq q\left[-\frac{\partial\phi}{\partial\mathbf{x}}\bigg|_i + (\beta_b c\hat{\mathbf{z}} + \delta\mathbf{v}_i) \times \left(\frac{\partial}{\partial\mathbf{x}} \times \hat{\mathbf{z}}\frac{\beta_b}{c}\phi\right)\bigg|_i\right]$$

Resolve into transverse (x and y) and longitudinal (z) components and simplify:

$$\beta_b c\hat{\mathbf{z}} \times \left(\frac{\partial}{\partial\mathbf{x}} \times \hat{\mathbf{z}}\frac{\beta_b}{c}\phi\right)\bigg|_i = \beta_b^2\hat{\mathbf{z}} \times \left(\frac{\partial}{\partial\mathbf{x}_\perp} \times \hat{\mathbf{z}}\phi\right)\bigg|_i$$

$$= \beta_b^2\hat{\mathbf{z}} \times \left(\frac{\partial\phi}{\partial y}\hat{\mathbf{x}} - \frac{\partial\phi}{\partial x}\hat{\mathbf{y}}\right)\bigg|_i$$

$$= \beta_b^2\left(\frac{\partial\phi}{\partial x}\hat{\mathbf{x}} + \frac{\partial\phi}{\partial y}\hat{\mathbf{y}}\right)\bigg|_i$$

$$= \beta_b^2\frac{\partial\phi}{\partial\mathbf{x}_\perp}\bigg|_i$$

also

$$-\frac{\partial\phi}{\partial\mathbf{x}}\bigg|_i = -\frac{\partial\phi}{\partial\mathbf{x}_\perp}\bigg|_i - \frac{\partial\phi}{\partial\mathbf{z}}\bigg|_i\hat{\mathbf{z}}$$

Together, these results give:

$$\mathbf{F}_i^s = \underbrace{-\frac{q}{\gamma_b^2}\frac{\partial\phi}{\partial\mathbf{x}_\perp}\bigg|_i}_{\text{Transverse}} \quad \underbrace{-\hat{\mathbf{z}}q\frac{\partial\phi}{\partial z}\bigg|_i}_{\text{Longitudinal}}$$

$$\gamma_b \equiv \frac{1}{\sqrt{1-\beta_b^2}} \qquad \text{Axial relativistic gamma of beam}$$

- Transverse and longitudinal forces have different axial gamma factors
- $1/\gamma_b^2$ factor in transverse force shows the space-charge forces become weaker as axial beam kinetic energy increases
  - Most important in low energy (nonrelativistic) beam transport
  - Strong in/near injectors before much acceleration

/// Aside: Singular Self Fields

In *free space*, the beam potential generated from the singular charge density:

$$\rho^s = \sum_{i=1}^N q_i\delta[\mathbf{x} - \mathbf{x}_i(t)]$$

is

$$\phi(\mathbf{x}) = \frac{q}{4\pi\epsilon_0}\sum_{i=1}^N \frac{1}{|\mathbf{x} - \mathbf{x}_i|}$$

Thus, the force of a particle at $\mathbf{x} = \mathbf{x}_i$ is:

$$\mathbf{F}_i = -q\frac{\partial\phi}{\partial\mathbf{x}}\bigg|_i = \frac{q^2}{4\pi\epsilon_0}\sum_{j=1}^N \frac{(\mathbf{x}_i - \mathbf{x}_j)}{|\mathbf{x}_i - \mathbf{x}_j|^{3/2}}$$

Which diverges due to the $i = j$ term. This divergence is essentially "erased" when the continuous charge density is applied:

$$\rho^s = \sum_{i=1}^N q_i\delta[\mathbf{x} - \mathbf{x}_i(t)] \quad \longrightarrow \quad \rho(\mathbf{x}, t)$$

- Effectively removes effect of collisions

  See: J.J. Barnard, Intro Lectures for more details

  - Find collisionless Vlasov model of evolution is often adequate

///

The particle equations of motion in $\mathbf{x}_i - \mathbf{v}_i$ phase-space variables become:

- Separate parts of $q\mathbf{E}_i^a + q\mathbf{v}_i \times \mathbf{B}_i^a$ into transverse and longitudinal comp

Transverse

$$\frac{d}{dt}\mathbf{x}_{\perp i} = \mathbf{v}_{\perp i}$$

$$\frac{d}{dt}(m\gamma_i\mathbf{v}_{\perp i}) \simeq \underbrace{q\mathbf{E}_{\perp i}^a + q\beta_b c\hat{\mathbf{z}} \times \mathbf{B}_{\perp i}^a + qB_{zi}^a\mathbf{v}_{\perp i} \times \hat{\mathbf{z}}}_{\text{Applied}} \underbrace{- q\frac{1}{\gamma_b^2}\frac{\partial\phi}{\partial\mathbf{x}_\perp}\bigg|_i}_{\text{Self}}$$

Longitudinal

$$\frac{d}{dt}z_i = v_{zi}$$

$$\frac{d}{dt}(m\gamma_i v_{zi}) \simeq \underbrace{qE_{zi}^a - q(v_{xi}B_{yi}^a - v_{yi}B_{xi}^a)}_{\text{Applied}} \underbrace{- q\frac{\partial\phi}{\partial z}\bigg|_i}_{\text{Self}}$$

In the remainder of this (and most other) lectures, we analyze Transverse Dynamics. Longitudinal Dynamics will be covered in J.J. Barnard lectures

- Except near injector, acceleration is typically slow
  - Fractional change in γ_b, β_b small over characteristic transverse dynamical scales such as lattice period and betatron oscillation periods
- Regard γ_b, β_b as specified functions given by the "acceleration schedule"

S1E: Equations of Motion in s and the Paraxial Approximation

In transverse accelerator dynamics, it is convenient to employ the axial coordinate (s) of a particle in the accelerator as the independent variable:

- Need fields at lattice location of particle to integrate equations for particle trajectories

$$s \equiv s_i + \int_{t_i}^{t} d\tilde{t}\; v_{zi}(\tilde{t})$$

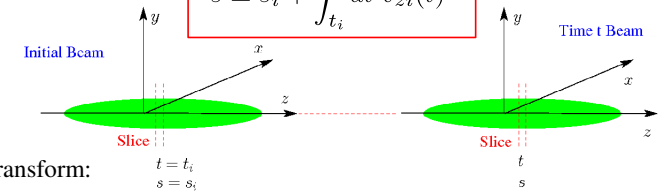

Transform:

$$v_{zi} = \frac{ds}{dt} \quad \Longrightarrow \quad v_{xi} = \frac{dx_i}{dt} = \frac{ds}{dt}\frac{dx_i}{ds} = v_{zi}\frac{dx_i}{ds} = (\beta_b c + \delta v_{zi})\frac{dx_i}{ds} \simeq \beta_b c \frac{dx_i}{ds}$$

Neglect

Denote:

$$' \equiv \frac{d}{ds} \qquad v_{xi} = \frac{dx_i}{dt} \simeq \beta_b c x_i' \qquad v_{yi} = \frac{dy_i}{dt} \simeq \beta_b c y_i'$$

Neglecting term consistent with assumption of small longitudinal momentum spread (paraxial approximation)

- Procedure becomes more complicated when bends present: see S1H

In the paraxial approximation, x' and y' can be interpreted as the (small magnitude) angles that the particles make with the longitudinal-axis:

$$x - \text{angle} = \frac{v_{xi}}{v_{zi}} \simeq \frac{v_{xi}}{\beta_b c} = x_i' \qquad y - \text{angle} = \frac{v_{yi}}{v_{zi}} \simeq \frac{v_{yi}}{\beta_b c} = y_i'$$

Typical accel lattice values: $|x'| < 50$ mrad

The angles will be *small* in the paraxial approximation:

$$v_{xi}^2,\; v_{yi}^2 \ll \beta_b^2 c^2 \quad \Longrightarrow \quad x_i'^2,\; y_i'^2 \ll 1$$

Since the spread of axial momentum/velocities is small in the paraxial approximation, a thin axial slice of the beam maps to a thin axial slice and s can also be thought of as the axial coordinate of the slice in the accelerator lattice

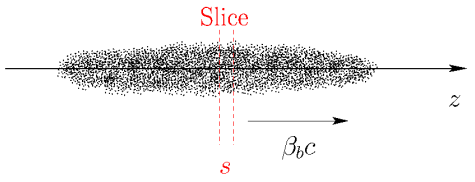

$$\beta_b \equiv \sum_{i=1}^{N'} \frac{v_{zi}}{c}$$

slice

$$s \simeq s_i + \int_{t_i}^{t} d\tilde{t}\; \beta_b(\tilde{t})$$

$$s \simeq s_i + \int_{t_i}^{t} d\tilde{t}\; \beta_b(\tilde{t})$$

The coordinate s can alternatively be interpreted as the axial coordinate of a reference (design) particle moving in the lattice

- Design particle has no momentum spread

It is often desirable to express the particle equations of motion in terms of s rather than the time t

- Makes it clear where you are in the lattice of the machine
- Sometimes easier to use t in codes when including many effects to high order

Transform transverse particle equations of motion to s rather than t derivatives

$$\frac{d}{dt}(m\gamma_i \mathbf{v}_{\perp i}) \simeq q\mathbf{E}_{\perp i}^a + q\beta_b c\hat{\mathbf{z}} \times \mathbf{B}_{\perp i}^a + qB_{zi}^a \mathbf{v}_{\perp i} \times \hat{\mathbf{z}} - q\frac{1}{\gamma_b^2}\left.\frac{\partial \phi}{\partial \mathbf{x}_\perp}\right|_i$$

Term 1 Term 2

Transform Terms 1 and 2 in the particle equation of motion:

$$\frac{d}{dt} = v_{zi}\frac{d}{ds}$$

Term 1: $$\frac{d}{dt}\left(m\gamma_i \frac{d\mathbf{x}_{\perp i}}{dt}\right) = mv_{zi}\frac{d}{ds}\left(\gamma_i v_{zi}\frac{d}{ds}\mathbf{x}_{\perp i}\right) = m\gamma_i v_{zi}^2 \frac{d^2}{ds^2}\mathbf{x}_{\perp i} + mv_{zi}\left(\frac{d}{ds}\mathbf{x}_{\perp i}\right)\frac{d}{ds}(\gamma_i v_{zi})$$

Term 1A Term 1B

Approximate:

Term 1A: $$m\gamma_i v_{zi}^2 \frac{d^2}{ds^2}\mathbf{x}_{\perp i} \simeq m\gamma_b \beta_b^2 c^2 \frac{d^2}{ds^2}\mathbf{x}_{\perp i} = m\gamma_b \beta_b^2 c^2 \mathbf{x}_{\perp i}''$$

Term 1B: $$mv_{zi}\left(\frac{d}{ds}\mathbf{x}_{\perp i}\right)\frac{d}{ds}(\gamma_i v_{zi}) \simeq m\beta_b c\left(\frac{d}{ds}\mathbf{x}_{\perp i}\right)\frac{d}{ds}(\gamma_b \beta_b c) \simeq m\beta_b c^2 (\gamma_b \beta_b)' \mathbf{x}_{\perp i}'$$

Using the approximations 1A and 1B gives for Term 1:

$$m\frac{d}{dt}\left(\gamma_i\frac{d\mathbf{x}_{\perp i}}{dt}\right) \simeq m\gamma_b\beta_b^2c^2\left[\mathbf{x}''_{\perp i} + \frac{(\gamma_b\beta_b)'}{(\gamma_b\beta_b)}\mathbf{x}'_{\perp i}\right]$$

Similarly we approximate in Term 2:

$$qB^a_{zi}\mathbf{v}_{\perp i}\times\hat{\mathbf{z}} \simeq qB^a_{zi}\beta_b c\mathbf{x}'_{\perp i}\times\hat{\mathbf{z}}$$

Using the simplified expressions for Terms 1 and 2 obtain the reduced transverse equation of motion:

$$\mathbf{x}''_{\perp i} + \frac{(\gamma_b\beta_b)'}{(\gamma_b\beta_b)}\mathbf{x}'_{\perp i} = \frac{q}{m\gamma_b\beta_b^2c^2}\mathbf{E}^a_{\perp i} + \frac{q}{m\gamma_b\beta_b c}\hat{\mathbf{z}}\times\mathbf{B}^a_{\perp i} + \frac{qB^a_{zi}}{m\gamma_b\beta_b c}\mathbf{x}'_{\perp i}\times\hat{\mathbf{z}} - \frac{q}{m\gamma_b^3\beta_b^2c^2}\left.\frac{\partial\phi}{\partial\mathbf{x}_\perp}\right|_i$$

- Will be analyzed extensively in lectures that follow in various limits to better understand solution properties

S1F: Axial Particle Kinetic Energy

Relativistic particle kinetic energy is:

$$\mathcal{E} = (\gamma - 1)mc^2$$

$$\gamma = \frac{1}{\sqrt{1-\mathbf{v}^2/c^2}}$$

$$\mathbf{v} = (\beta_b + \delta\beta_z)c\hat{\mathbf{z}} + \beta_\perp c\hat{\mathbf{x}}_\perp = \text{Particle Velocity (3D)}$$

For a directed paraxial beam with motion primarily along the machine axis the kinetic energy is essentially the axial kinetic energy $\mathcal{E}_b$:

$$\mathcal{E} = (\gamma_b - 1)mc^2 + \Theta\left(\frac{|\delta\beta_z|}{\beta_b}, \frac{\beta_\perp^2}{\beta_b^2}\right)$$

$$\mathcal{E} \simeq \mathcal{E}_b \equiv (\gamma_b - 1)mc^2$$

In nonrelativistic limit: $\beta_b^2 \ll 1$

$$\mathcal{E}_b \equiv (\gamma_b - 1)mc^2 = \frac{1}{2}m\beta_b^2c^2 + \frac{3}{8}m\beta_b^4c^2 + \cdots \simeq \frac{1}{2}m\beta_b^2c^2 + \Theta(\beta_b^4)$$

Convenient units:

Electrons:

$$m = m_e = 511\ \frac{\text{keV}}{c^2}$$

Electrons rapidly relativistic due to relatively low mass

Ions/Protons:

$$m = (\text{atomic mass})\cdot m_u \qquad m_u \equiv \text{Atomic Mass Unit} = 931.49\ \frac{\text{MeV}}{c^2}$$

Note:

$$m_p = \text{Proton Mass} = 938.27\ \frac{\text{MeV}}{c^2}$$

$$m_n = \text{Neutron Mass} = 939.57\ \frac{\text{MeV}}{c^2}$$

$$m_p \simeq m_n \simeq 940\frac{\text{MeV}}{c^2}$$

Approximate roughly for ions:

$$m \simeq Am_u \qquad A = \text{Mass Number (Number of Nucleons)}$$

$m_u \gg m_e$

Protons/ions take much longer to become relativistic than electrons

$m_p, m_n > m_u$ due to nuclear binding energy

$$\frac{\mathcal{E}_b/A}{m_uc^2} \simeq \gamma_b - 1 \implies \gamma_b = 1 + \frac{\mathcal{E}_b/A}{m_uc^2}, \quad \beta_b = \sqrt{1-1/\gamma_b^2}$$

Energy/Nucleon $\mathcal{E}_b/A$ fixes β_b to set phase needs of RF cavities

Contrast beam relativistic β_b for electrons and protons/ions:

Electrons

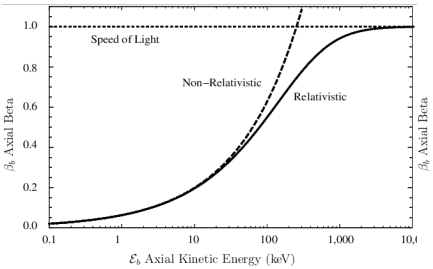

Ions (and approx Protons)

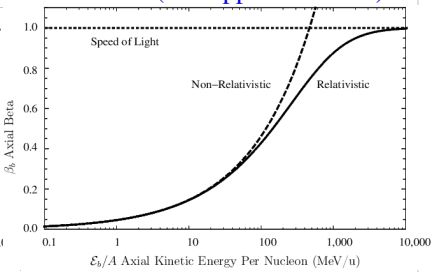

Notes: 1) plots do not overlay, scale changed
2) Ion plot slightly off for protons since $m_u \neq m_p$

- Electrons become relativistic easier relative to protons/ions due to light mass
- Space-charge more important for ions than electrons (see Sec. S1D)
  - Low energy ions near injector expected to have strongest space-charge

S1G: Summary: Transverse Particle Equations of Motion

$$\mathbf{x}''_\perp + \frac{(\gamma_b\beta_b)'}{(\gamma_b\beta_b)}\mathbf{x}'_\perp = \frac{q}{m\gamma_b\beta_b^2c^2}\mathbf{E}^a_\perp + \frac{q}{m\gamma_b\beta_b c}\hat{\mathbf{z}}\times\mathbf{B}^a_\perp + \frac{qB^a_z}{m\gamma_b\beta_b c}\mathbf{x}'_\perp\times\hat{\mathbf{z}} - \frac{q}{m\gamma_b^3\beta_b^2c^2}\frac{\partial}{\partial\mathbf{x}_\perp}\phi$$

$\mathbf{E}^a$ = Applied Electric Field

$\mathbf{B}^a$ = Applied Magnetic Field

$$\prime \equiv \frac{d}{ds} \qquad \gamma_b \equiv \frac{1}{\sqrt{1-\beta_b^2}}$$

$$\nabla^2\phi = \frac{\partial}{\partial\mathbf{x}}\cdot\frac{\partial}{\partial\mathbf{x}}\phi = -\frac{\rho}{\epsilon_0}$$

+ Boundary Conditions on ϕ

Drop particle *i* subscripts (in most cases) henceforth to simplify notation

Neglects axial energy spread, bending, and electromagnetic radiation

$\gamma-$ factors different in applied and self-field terms:

In $-\frac{q}{m\gamma_b^3\beta_b^2c^2}\frac{\partial}{\partial\mathbf{x}}\phi$, contributions to γ_b^3 :

$\gamma_b \Longrightarrow$ Kinematics

$\gamma_b^2 \Longrightarrow$ Self-Magnetic Field Corrections (leading order)

S1H: Preview: Analysis to Come

Much of transverse accelerator physics centers on understanding the evolution of beam particles in 4-dimensional *x*-*x*' and *y*-*y*' phase space.

Typically, restricted 2-dimensional phase-space projections in *x*-*x*' and/or *y*-*y*' are analyzed to simplify interpretations:

When forces are linear particles tend to move on ellipses of constant area
- Ellipse may elongate/shrink and rotate as beam evolves in lattice

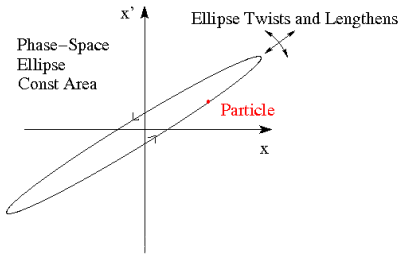

Nonlinear force components distort orbits and cause undesirable effects
- Growth in effective phase-space area reduces focusability

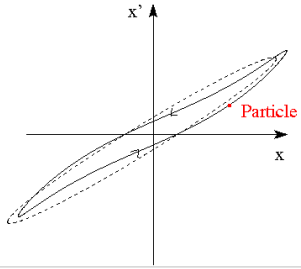

The "effective" phase-space volume of a distribution of beam particles is of fundamental interest

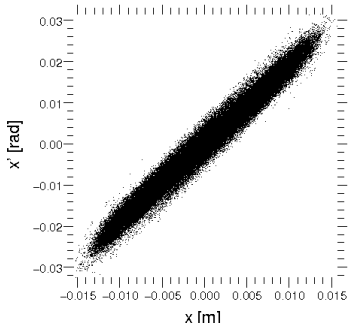

Effective area measure in *x*-*x*' phase-space is the *x*-emittance

Statistical "Area" $\sim \pi\varepsilon_x$

$$\varepsilon_x = 4[\langle x^2\rangle_\perp\langle x'^2\rangle_\perp - \langle xx'\rangle_\perp^2]^{1/2}$$

We will find in statistical beam descriptions that:

Larger/Smaller beam phase-space areas (Larger/Smaller emittances) $\Longleftrightarrow$ Harder/Easier to focus beam on small final spots

Much of advanced accelerator physics centers on preserving beam quality by understanding and controlling emittance growth due to nonlinear forces arising from both space-charge and the applied focusing. In the remainder of the next few lectures we will review the physics of a single particles moving in linear applied fields with emphasis on transverse effects. Later, we will generalize concepts to include forces from space-charge in this formulation and nonlinear effects from both applied and self-fields.

S1I: Bent Coordinate System and Particle Equations of Motion with Dipole Bends and Axial Momentum Spread

The previous equations of motion can be applied to dipole bends provided the *x,y,z* coordinate system is fixed. It can prove more convenient to employ coordinates that follow the beam in a bend.

- Orthogonal system employed called Frenet-Serret coordinates

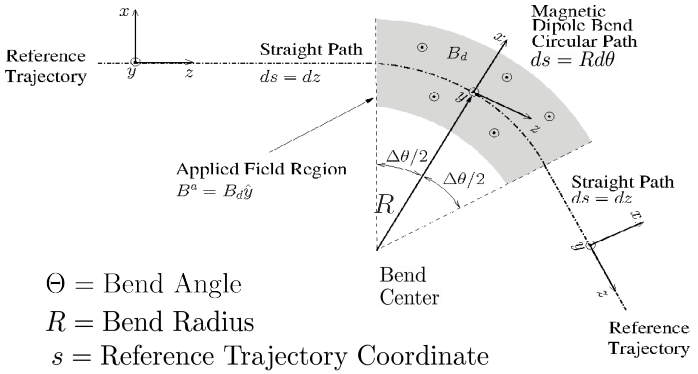

In this perspective, dipoles are adjusted given the design momentum of the reference particle to bend the orbit through a radius *R*.

- Bends usually only in one plane (say *x*)
  - Implemented by a dipole applied field: E_x^a or B_y^a
- Easy to apply material analogously for *y*-plane bends, if necessary

Denote:

$$p_0 = m\gamma_b\beta_b c = \text{design momentum}$$

Then a magnetic *x*-bend through a radius *R* is specified by:

$$\mathbf{B}^a = B_y^a\hat{\mathbf{y}} = \text{const in bend}$$
$$\frac{1}{R} = \frac{qB_y^a}{p_0}$$

Analogous formula for Electric Bend will be derived in problem set

The particle rigidity is defined as ($[B\rho]$ read as one symbol called "B-Rho"):

$$[B\rho] \equiv \frac{p_0}{q} = \frac{m\gamma_b\beta_b c}{q}$$

is often applied to express the bend result as:

$$\frac{1}{R} = \frac{B_y^a}{[B\rho]}$$

Comments on bends:

- *R* can be positive or negative depending on sign of $B_y^a/[B\rho]$
- For straight sections, $R \to \infty$ (or equivalently, $B_y^a = 0$)
- Lattices often made from discrete element dipoles and straight sections with separated function optics
  - Bends can provide "edge focusing"
  - Sometimes elements for bending/focusing are combined
- For a ring, dipoles strengths are tuned with particle rigidity/momentum so the reference orbit makes a closed path lap through the circular machine
  - Dipoles adjusted as particles gain energy to maintain closed path
  - In a Synchrotron dipoles and focusing elements are adjusted together to maintain focusing and bending properties as the particles gain energy. This is the origin of the name "Synchrotron."
- Total bending strength of a ring in Tesla-meters limits the ultimately achievable particle energy/momentum in the ring

For a magnetic field over a path length *S* , the beam will be bent through an angle:

$$\Theta = \frac{S}{R} = \frac{SB_y^a}{[B\rho]}$$

To make a ring, the bends must deflect the beam through a total angle of 2π :

- Neglect any energy gain changing the rigidity over one lap

$$2\pi = \sum_{i,\text{Dipoles}} \Theta_i = \sum_i \frac{S_i}{R_i} = \sum_i \frac{S_i B_{y,i}^a}{[B\rho]}$$

For a symmetric ring, *N* dipoles are all the same, giving for the bend field:

- Typically choose parameters for dipole field as high as technology allows for a compact ring

$$B_y^a = 2\pi\frac{[B\rho]}{NS}$$

For a symmetric ring of total circumference *C* with straight sections of length *L* between the bends:

- Features of straight sections typically dictated by needs of focusing, acceleration, and dispersion control

$$C = NS + NL$$

Example: Typical separated function lattice in a Synchrotron

Focus Elements in Red

Bending Elements in Green

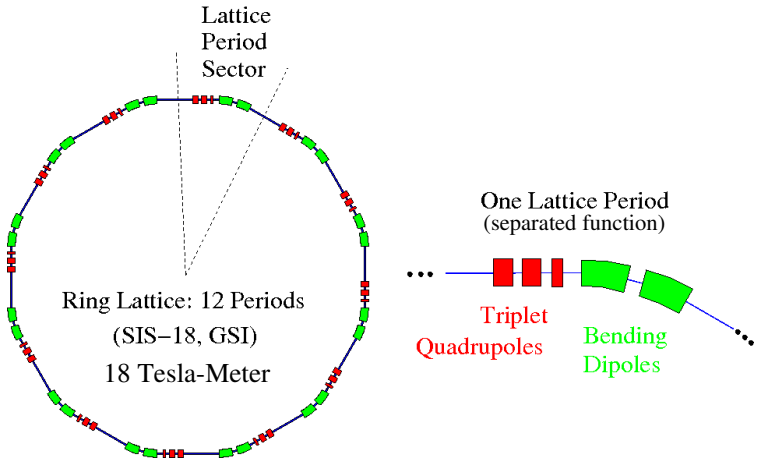

For "off-momentum" errors:

$$p_s = p_0 + \delta p$$
$$p_0 = m\gamma_b\beta_b c = \text{design momentum}$$
$$\delta p = \text{off- momentum}$$

This will modify the particle equations of motion, particularly in cases where there are bends since particles with different momenta will be bent at different radii

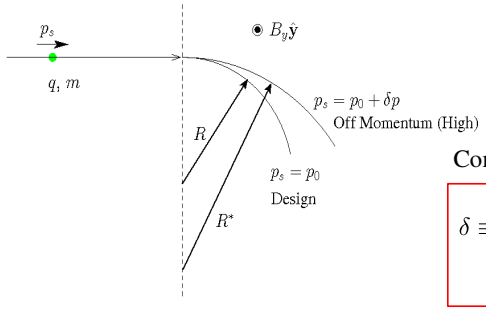

Common notation:

$$\delta \equiv \frac{\delta p}{p_0} = \text{Fractional Momentum Error}$$

- Not usual to have acceleration in bends
  - Dipole bends and quadrupole focusing are sometimes combined

Derivatives in accelerator Frenet-Serret Coordinates

Summarize results only needed to transform the Maxwell equations, write field derivatives, etc.

- Reference: Chao and Tigner, *Handbook of Accelerator Physics and Engineering*

$$\Psi(x,y,s) \qquad = \text{Scalar}$$
$$\mathbf{V}(x,y,s) = V_x(x,y,s)\hat{\mathbf{x}} + V_y(x,y,s)\hat{\mathbf{y}} + V_s(x,y,s)\hat{\mathbf{s}} \quad = \text{Vector}$$

Vector Dot and Cross-Products: ($\mathbf{V}_1$, $\mathbf{V}_2$ Two Vectors)

$$\mathbf{V}_1 \cdot \mathbf{V}_2 = V_{1x}V_{2x} + V_{1y}V_{2y} + V_{1s}V_{2s}$$

$$\mathbf{V}_1 \times \mathbf{V}_2 = \begin{vmatrix} \hat{\mathbf{x}} & \hat{\mathbf{y}} & \hat{\mathbf{s}} \\ V_{1x} & V_{1y} & V_{1s} \\ V_{2x} & V_{2y} & V_{2s} \end{vmatrix}$$
$$= (V_{1x}V_{2s} - V_{1s}V_{2x})\hat{\mathbf{x}} + (V_{1s}V_{2x} - V_{1x}V_{2s})\hat{\mathbf{y}} + (V_{1x}V_{2y} - V_{1y}V_{2x})\hat{\mathbf{s}}$$

Elements:

$$d^2x_\perp = dxdy$$
$$d^3x_\perp = \left(1 + \frac{x}{R}\right) dxdyds$$
$$d\vec{\ell} = \hat{\mathbf{x}}dx + \hat{\mathbf{y}}dy + \hat{\mathbf{s}}\left(1 + \frac{x}{R}\right) ds$$

Gradient:

$$\nabla\Psi = \hat{\mathbf{x}}\frac{\partial\Psi}{\partial x} + \hat{\mathbf{y}}\frac{\partial\Psi}{\partial y} + \hat{\mathbf{s}}\frac{1}{1+x/R}\frac{\partial\Psi}{\partial s}$$

Divergence:

$$\nabla\cdot\mathbf{V} = \frac{1}{1+x/R}\frac{\partial}{\partial x}\left[(1+x/R)V_x\right] + \frac{\partial V_y}{\partial y} + \frac{1}{1+x/R}\frac{\partial V_s}{\partial s}$$

Curl:

$$\nabla\times\mathbf{V} = \hat{\mathbf{x}}\left(\frac{\partial V_s}{\partial y} - \frac{1}{1+x/R}\frac{\partial V_y}{\partial s}\right) + \hat{\mathbf{y}}\frac{1}{1+x/R}\left(\frac{\partial V_x}{\partial s} - \frac{\partial}{\partial x}\left[(1+x/R)V_s\right]\right)$$
$$+ \hat{\mathbf{s}}(1+x/R)\left(\frac{\partial V_y}{\partial x} - \frac{\partial V_x}{\partial y}\right)$$

Laplacian:

$$\nabla^2\Psi = \frac{1}{1+x/R}\frac{\partial}{\partial x}\left[\left(1+\frac{x}{R}\right)\frac{\partial\Psi}{\partial x}\right] + \frac{\partial^2\Psi}{\partial y^2} + \frac{1}{1+x/R}\frac{\partial}{\partial s}\left[\frac{1}{1+x/R}\frac{\partial\Psi}{\partial s}\right]$$

Transverse particle equations of motion including bends and "off-momentum" effects

- See texts such as Edwards and Syphers for guidance on derivation steps
- Full derivation is beyond needs/scope of this class

$$x'' + \frac{(\gamma_b\beta_b)'}{(\gamma_b\beta_b)}x' + \left[\frac{1}{R^2(s)}\frac{1-\delta}{1+\delta}\right]x = \frac{\delta}{1+\delta}\frac{1}{R(s)} + \frac{q}{m\gamma_b\beta_b^2c^2}\frac{E_x^a}{(1+\delta)^2} - \frac{q}{m\gamma_b\beta_bc}\frac{B_y^a}{1+\delta} + \frac{q}{m\gamma_b\beta_bc}\frac{B_s^a}{1+\delta}y' - \frac{q}{m\gamma_b^3\beta_b^2c^2}\frac{1}{1+\delta}\frac{\partial\phi}{\partial x}$$

$$y'' + \frac{(\gamma_b\beta_b)'}{(\gamma_b\beta_b)}y' = \frac{q}{m\gamma_b\beta_b^2c^2}\frac{E_y^a}{(1+\delta)^2} + \frac{q}{m\gamma_b\beta_bc}\frac{B_x^a}{1+\delta} - \frac{q}{m\gamma_b\beta_bc}\frac{B_s^a}{1+\delta}x' - \frac{q}{m\gamma_b^3\beta_b^2c^2}\frac{1}{1+\delta}\frac{\partial\phi}{\partial y}$$

$p_0 = m\gamma_b\beta_bc =$ Design Momentum

$\delta \equiv \dfrac{\delta p}{p_0} =$ Fractional Momentum Error

$$\frac{1}{R(s)} = \frac{B_y^a(s)|_{\text{Dipole}}}{[B\rho]} \qquad [B\rho] = \frac{p_0}{q}$$

Comments:

- Design bends only in x and B_y^a, E_x^a contain <u>no</u> dipole terms (design orbit)
  - Dipole components set via the design bend radius $R(s)$
- Equations contain only low-order terms in momentum spread δ

Comments continued:

- Equations are often applied linearized in δ
- Achromatic focusing lattices are often designed using equations with momentum spread to obtain focal points independent of δ to some order
  x and y equations differ significantly due to bends modifying the x-equation when $R(s)$ is finite
- It will be shown in the problems that for electric bends:

$$\frac{1}{R(s)} = \frac{E_x^a(s)}{\beta_bc[B\rho]}$$

- Applied fields for focusing: $\mathbf{E}_\perp^a$, $\mathbf{B}_\perp^a$, B_s^a
  must be expressed in the bent x,y,s system of the reference orbit
  - Includes error fields in dipoles
- Self fields may also need to be solved taking into account bend terms
  - Often can be neglected in Poisson's Equation

$$\left\{\frac{1}{1+x/R}\frac{\partial}{\partial x}\left[\left(1+\frac{x}{R}\right)\frac{\partial}{\partial x}\right] + \frac{\partial^2}{\partial y^2} + \frac{1}{1+x/R}\frac{\partial}{\partial s}\left[\frac{1}{1+x/R}\frac{\partial}{\partial s}\right]\right\}\phi = -\frac{\rho}{\epsilon_0}$$

if $R \to \infty$

reduces to familiar: $\left\{\dfrac{\partial^2}{\partial x^2} + \dfrac{\partial^2}{\partial y^2} + \dfrac{\partial^2}{\partial s^2}\right\}\phi = -\dfrac{\rho}{\epsilon_0}$

Appendix A: Gamma and Beta Factor Conversions

It is frequently the case that functions of the relativistic gamma and beta factors are converted to superficially different appearing forms when analyzing transverse particle dynamics in order to more cleanly express results. Here we summarize useful formulas in that come up when comparing various forms of equations. Derivatives are taken wrt the axial coordinate s but also apply wrt time t

Results summarized here can be immediately applied in the paraxial approximation by taking:

$$v = |\mathbf{v}| \simeq v_b = \beta_bc \implies \begin{aligned}\beta &\simeq \beta_b \\ \gamma &\simeq \gamma_b\end{aligned}$$

Assume that the beam is forward going with $\beta \geq 0$:

$$\gamma \equiv \frac{1}{\sqrt{1-\beta^2}} \qquad \beta = \frac{1}{\gamma}\sqrt{\gamma^2-1}$$

$$\gamma^2 = \frac{1}{1-\beta^2} \qquad \beta^2 = 1 - 1/\gamma^2$$

A commonly occurring acceleration factor can be expressed in several ways:

- Depending on choice used, equations can look quite different!

$$\frac{(\gamma\beta)'}{(\gamma\beta)} = \frac{\gamma'}{\gamma} + \frac{\beta'}{\beta} = \frac{\gamma'}{\gamma\beta^2}$$

Axial derivative factors can be converted using:

$$\gamma' = \frac{\beta\beta'}{(1-\beta^2)^{3/2}} \qquad \beta' = \frac{\gamma'}{\gamma^2\sqrt{\gamma^2-1}}$$

Energy factors:

$$\mathcal{E}_{\text{tot}} = \gamma mc^2 = \mathcal{E} + mc^2$$

$$\gamma\beta = \sqrt{\left(\frac{\mathcal{E}}{mc^2}\right)^2 + 2\left(\frac{\mathcal{E}}{mc^2}\right)}$$

Rigidity:

$$[B\rho] = \frac{p}{q} = \frac{\gamma mv}{q} = \frac{mc}{q}\gamma\beta = \frac{mc}{q}\sqrt{\left(\frac{\mathcal{E}}{mc^2}\right)^2 + 2\left(\frac{\mathcal{E}}{mc^2}\right)}$$

Appendix B: Magnetic Self-Fields

The full Maxwell equations for the beam self fields

$\mathbf{E}^s, \quad \mathbf{B}^s$

with electromagnetic effects neglected can be written as

- Good approx typically for slowly varying ions in weak fields

$$\nabla \cdot \mathbf{E}^s = \frac{\rho}{\epsilon_0} \qquad \nabla \times \mathbf{B}^s = \mu_0 \mathbf{J} + \frac{1}{c^2}\frac{\partial}{\partial t}\mathbf{E}^s$$

$$\nabla \times \mathbf{E}^s = -\frac{\partial}{\partial t}\mathbf{B}^s \qquad \nabla \cdot \mathbf{B}^s = 0$$

$+$ Boundary Conditions on $\mathbf{E}^s$ and $\mathbf{B}^s$ from material structures, etc.

$$\rho = qn(\mathbf{x},t) \qquad n(\mathbf{x},t) = \text{Number Density}$$

$$\mathbf{J} = qn(\mathbf{x},t)\mathbf{V}(\mathbf{x},t) \qquad \mathbf{V}(\mathbf{x},t) = \text{"Fluid" Flow Velocity}$$

- Beam terms from charged particles making up the beam
- Calc from continuum approx distribution

Electrostatic Approx:

$$\nabla \cdot \mathbf{E}^s = \frac{qn}{\epsilon_0} \qquad \nabla \times \mathbf{E}^s = 0$$

$$\mathbf{E}^s = -\nabla\phi$$

$\phi =$ Electrostatic Scalar Potential

$$\Longrightarrow \quad \nabla \times \mathbf{E}^s = -\nabla \times \nabla\phi = 0$$

Continuity of mixed partial derivatives

$$\Longrightarrow \quad \nabla \cdot \mathbf{E}^s = -\nabla \cdot \nabla\phi = \frac{qn}{\epsilon_0}$$

$$\nabla^2\phi = -\frac{qn}{\epsilon_0}$$

$+$ Boundary Conditions on ϕ

Magnetostatic Approx:

$$\nabla \times \mathbf{B}^s = \mu_0 \mathbf{J} \qquad \nabla \cdot \mathbf{B}^s = 0$$

$$\mathbf{B}^s = \nabla \times \mathbf{A}$$

$\mathbf{A} =$ Magnetostatic Vector Potential

$$\Longrightarrow \quad \nabla \cdot \mathbf{B}^s = \nabla \cdot (\nabla \times \mathbf{A}) = 0$$

Continuity of mixed partial derivatives

$$\Longrightarrow \quad \nabla \times \mathbf{B}^s = \nabla \times (\nabla \times \mathbf{A}) = \mu_0 \mathbf{J}$$

Continue next slide

Magnetostatic Approx Continued:

$$\nabla \times \mathbf{B}^s = \nabla \times (\nabla \times \mathbf{A}) = \mu_0 \mathbf{J}$$

$$\nabla(\nabla \cdot \mathbf{A}) - \nabla^2 \mathbf{A} = \mu_0 \mathbf{J}$$

Still free to take (gauge choice):

$$\nabla \cdot \mathbf{A} = 0 \quad \text{Coulomb Gauge}$$

Can always meet this choice:

$$\mathbf{A} \to \mathbf{A} + \nabla\xi \qquad \xi = \text{Some Function}$$

$$\Longrightarrow \quad \mathbf{B}^s = \nabla \times \mathbf{A} \to \nabla \times \mathbf{A} + \nabla \times \nabla\xi = \nabla \times \mathbf{A}$$

($\nabla\xi \to 0$ Cont mixed partial derivatives)

$$\Longrightarrow \nabla \cdot \mathbf{A} \to \nabla \cdot \mathbf{A} + \nabla^2\xi$$

Can always choose ξ such that $\nabla \cdot \mathbf{A} = 0$ to satisfy the Coulomb gauge:

$$\nabla^2 \mathbf{A} = -\mu_0 \mathbf{J} = -\mu_0 qn\mathbf{V}$$

$+$ Boundary Conditions on $\mathbf{A}$

- Essentially one Poisson form eqn for each field *x,y,z* comp
- Boundary conditions diff than ϕ

But can approximate this further for "typical" paraxial beams …..

$$\nabla^2 \mathbf{A} = -\mu_0 \mathbf{J} = -\mu_0 qn\mathbf{V}$$

Expect for a beam with primarily forward (paraxial) directed motion:

$$V_z = \beta_b c \qquad V_{x,y} \sim R'\beta_b c \qquad R' = \text{Beam Envelope Angle (Typically 10s mrad Magnitude)}$$

$$\Longrightarrow \quad |A_{x,y}| \ll |A_z|$$

Giving:

$$\nabla^2 A_z = -\mu_0 q \beta_b c n \qquad n = -\frac{\epsilon_0}{q}\nabla^2\phi$$

Free to use from electrostatic part

$$\nabla^2 A_z = -(\mu_0\epsilon_0) c \beta_b \nabla^2 \phi \qquad \mu_0\epsilon_0 = \frac{1}{c^2}$$

From unit definition

$$\Longrightarrow A_z = \frac{\beta_b}{c}\phi$$

- Allows simply taking into account low-order self-magnetic field effects
  - Care must be taken if magnetic materials are present close to beam

Further insight can be obtained on the nature of the approximations in the reduced form of the self-magnetic field correction by examining
Lorentz Transformation properties of the potentials.

From EM theory, the potentials $\phi,\ c\mathbf{A}$ form a relativistic 4-vector that transforms as a Lorentz vector for covariance:

$$A_\mu = (\phi,\ c\mathbf{A})$$

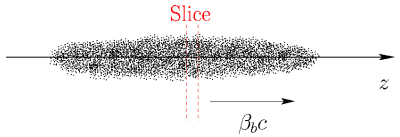

In the rest frame (*) of the beam, assume that the flows are small enough where the potentials are purely electrostatic with:

$$A^*_\mu = (\phi^*, \mathbf{0}) \qquad \nabla^2\phi^* = -\frac{qn^*}{\epsilon_0}$$

Review: Under Lorentz transform, the 4-vector components of $A_\mu = (\phi, c\mathbf{A})$ transform as the familiar 4-vector $x_\mu = (ct, \mathbf{x})$

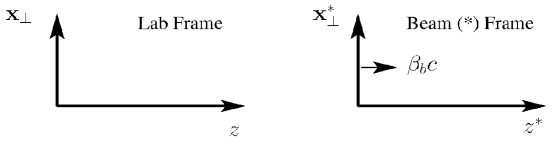

Transform

$$ct^* = \gamma_b(ct - \beta_b z)$$
$$z^* = \gamma_b(z - \beta_b ct)$$
$$\mathbf{x}^* = \mathbf{x}_\perp$$

Inverse Transform

$$ct = \gamma_b(ct^* + \beta_b z^*)$$
$$z = \gamma_b(z^* + \beta_b ct^*)$$
$$\mathbf{x} = \mathbf{x}^*_\perp$$

This gives for the 4-potential $A_\mu = (\phi, c\mathbf{A})$:

$$\phi = \gamma_b(\phi^* + \beta_b c\overbrace{A^*_z}^{0}) = \gamma_b\phi^*$$
$$cA_z = \gamma_b(c\overbrace{A^*_z}^{0} + \beta_b\phi^*) = \beta_b(\gamma_b\phi^*) = \beta_b\phi$$
$$\Longrightarrow \boxed{A_z = \frac{\beta_b}{c}\phi}$$

- Shows result is consistent with pure electrostatic in beam (*) frame

S2: Transverse Particle Equations of Motion in Linear Applied Focusing Channels

S2A: Introduction

Write out transverse particle equations of motion in explicit component form:

$$x'' + \frac{(\gamma_b\beta_b)'}{(\gamma_b\beta_b)}x' = \frac{q}{m\gamma_b\beta_b^2c^2}E^a_x - \frac{q}{m\gamma_b\beta_b c}B^a_y + \frac{q}{m\gamma_b\beta_b c}B^a_z y' - \frac{q}{m\gamma_b^3\beta_b^2c^2}\frac{\partial\phi}{\partial x}$$

$$y'' + \frac{(\gamma_b\beta_b)'}{(\gamma_b\beta_b)}y' = \frac{q}{m\gamma_b\beta_b^2c^2}E^a_y + \frac{q}{m\gamma_b\beta_b c}B^a_x - \frac{q}{m\gamma_b\beta_b c}B^a_z x' - \frac{q}{m\gamma_b^3\beta_b^2c^2}\frac{\partial\phi}{\partial y}$$

Equations previously derived under assumptions:

- No bends (fixed *x*-*y*-*z* coordinate system with no local bends)
- Paraxial equations ($x'^2, y'^2 \ll 1$)
- No dispersive effects (β_b same all particles), acceleration allowed ($\beta_b \neq$ const)
- Electrostatic and leading-order (in β_b) self-magnetic interactions

The applied focusing fields

Electric: $E^a_x,\ E^a_y$

Magnetic: $B^a_x,\ B^a_y,\ B^a_z$

must be specified as a function of *s* and the transverse particle coordinates *x* and *y* to complete the description

- Consistent change in axial velocity ($\beta_b c$) due to E^a_z must be evaluated
  - Typically due to RF cavities and/or induction cells
- Restrict analysis to fields from applied focusing structures

Intense beam accelerators and transport lattices are designed to optimize *linear* applied focusing forces with terms:

Electric:
$$E^a_x \simeq (\text{function of } s) \times (x \text{ or } y)$$
$$E^a_y \simeq (\text{function of } s) \times (x \text{ or } y)$$

Magnetic:
$$B^a_x \simeq (\text{function of } s) \times (x \text{ or } y)$$
$$B^a_y \simeq (\text{function of } s) \times (x \text{ or } y)$$
$$B^a_z \simeq (\text{function of } s)$$

Common situations that realize these linear applied focusing forms will be overviewed:

Continuous Focusing (see: S2B)
Quadrupole Focusing
- Electric (see: S2C)
- Magnetic (see: S2D)
Solenoidal Focusing (see: S2E)

Other situations that will not be covered (typically more nonlinear optics):

Einzel Lens (see: J.J. Barnard, Intro Lectures)
Plasma Lens
Wire guiding

Why design around linear applied fields ?

- Linear oscillators have well understood physics allowing formalism to be developed that can guide design
- Linear fields are "lower order" so it should be possible for a given source amplitude to generate field terms with greater strength than for "higher order" nonlinear fields

S2B: Continuous Focusing

Assume constant electric field applied focusing force:

$$\mathbf{B}^a = 0$$
$$\mathbf{E}^a_\perp = E^a_x\hat{\mathbf{x}} + E^a_y\hat{\mathbf{y}} = -\frac{m\gamma_b\beta_b^2c^2k_{\beta0}^2}{q}\mathbf{x}_\perp \qquad k_{\beta0}^2 \equiv \text{const} > 0$$
$$[k_{\beta0}] = \frac{\text{rad}}{\text{m}}$$

Continuous focusing equations of motion:

Insert field components into linear applied field equations and collect terms

$$\mathbf{x}''_\perp + \frac{(\gamma_b\beta_b)'}{(\gamma_b\beta_b)}\mathbf{x}'_\perp + k_{\beta0}^2\mathbf{x}_\perp = -\frac{q}{m\gamma_b^3\beta_b^2c^2}\frac{\partial\phi}{\partial\mathbf{x}_\perp}$$

$$x'' + \frac{(\gamma_b\beta_b)'}{(\gamma_b\beta_b)}x' + k_{\beta0}^2x = -\frac{q}{m\gamma_b^3\beta_b^2c^2}\frac{\partial\phi}{\partial x}$$
$$y'' + \frac{(\gamma_b\beta_b)'}{(\gamma_b\beta_b)}y' + k_{\beta0}^2y = -\frac{q}{m\gamma_b^3\beta_b^2c^2}\frac{\partial\phi}{\partial y}$$

Equivalent Component Form

Even this simple model can become complicated

- Space charge: ϕ must be calculated consistent with beam evolution
- Acceleration: acts to damp orbits (see: S10)

Simple model in limit of no acceleration ($\gamma_b\beta_b \simeq \text{const}$) and negligible space-charge ($\phi \simeq \text{const}$):

$$\mathbf{x}''_\perp + k_{\beta0}^2\mathbf{x}_\perp = 0 \quad \Longrightarrow \text{orbits simple harmonic oscillatons}$$

General solution is elementary:

$$\mathbf{x}_\perp = \mathbf{x}_\perp(s_i)\cos[k_{\beta0}(s-s_i)] + [\mathbf{x}'_\perp(s_i)/k_{\beta0}]\sin[k_{\beta0}(s-s_i)]$$
$$\mathbf{x}'_\perp = -k_{\beta0}\mathbf{x}_\perp(s_i)\sin[k_{\beta0}(s-s_i)] + \mathbf{x}'_\perp(s_i)\cos[k_{\beta0}(s-s_i)]$$
$$\mathbf{x}_\perp(s_i) = \text{ Initial coordinate}$$
$$\mathbf{x}'_\perp(s_i) = \text{ Initial angle}$$

In terms of a transfer map in the x-plane (y-plane analogous):

$$\begin{bmatrix} x \\ x' \end{bmatrix}_s = \mathbf{M}_x(s|s_i)\cdot\begin{bmatrix} x \\ x' \end{bmatrix}_{s_i}$$
$$\mathbf{M}_x(s|s_i) = \begin{bmatrix} \cos[k_{\beta0}(s-s_i)] & \frac{1}{k_{\beta0}}\sin[k_{\beta0}(s-s_i)] \\ -k_{\beta0}\sin[k_{\beta0}(s-s_i)] & \cos[k_{\beta0}(s-s_i)] \end{bmatrix}$$

/// Example: Particle Orbits in Continuous Focusing

Particle phase-space in x-x' with only applied field

$k_{\beta0} = 2\pi$ rad/m $\quad x(0) = 1$ mm $\quad y(0) = 0$
$\phi \simeq 0 \quad \gamma_b\beta_b = \text{const} \quad x'(0) = 0 \quad y'(0) = 0$

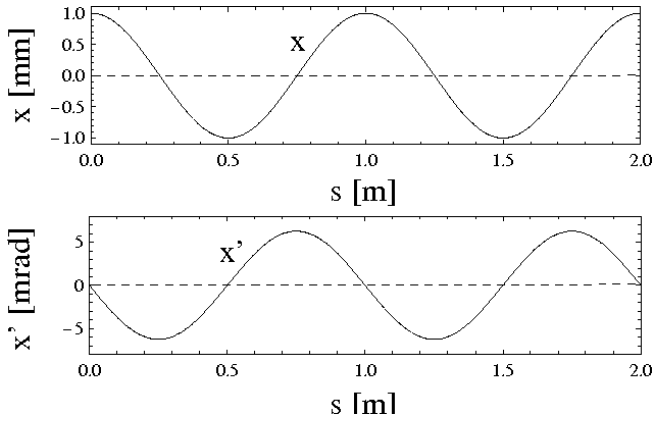

- Orbits in the applied field are just simple harmonic oscillators ///

Problem with continuous focusing model:

The continuous focusing model is realized by a stationary ($m \to \infty$) partially neutralizing uniform background of charges filling the beam pipe. To see this apply Maxwell's equations to the applied field to calculate an applied charge density:

$$\rho^a = \epsilon_0 \frac{\partial}{\partial \mathbf{x}} \cdot \mathbf{E}^a = -\frac{2m\epsilon_0\gamma_b\beta_b^2 c^2 k_{\beta 0}^2}{q} = \text{const}$$

- Unphysical model, but commonly employed since it represents the average action of more physical focusing fields in a simpler to analyze model
  - Demonstrate later in simple examples and problems given
- Continuous focusing can provide reasonably good estimates for more realistic periodic focusing models if $k_{\beta 0}^2$ is appropriately identified in terms of "equivalent" parameters *and* the periodic system is stable.
  - See lectures that follow and homework problems for examples

In more realistic models, one requires that *quasi-static* focusing fields in the machine aperture satisfy the vacuum Maxwell equations

$$\nabla \cdot \mathbf{E}^a = 0 \qquad \nabla \cdot \mathbf{B}^a = 0$$
$$\nabla \times \mathbf{E}^a = 0 \qquad \nabla \times \mathbf{B}^a = 0$$

- Require in the region of the beam
- Applied field sources outside of the beam region

The vacuum Maxwell equations constrain the 3D form of applied fields resulting from spatially localized lenses. The following cases are commonly exploited to optimize linear focusing strength in physically realizable systems while keeping the model relatively simple:

1) Alternating Gradient Quadrupoles with transverse orientation
   - Electric Quadrupoles (see: S2C)
   - Magnetic Quadrupoles (see: S2D)
2) Solenoidal Magnetic Fields with longitudinal orientation (see: S2E)
3) Einzel Lenses (see J.J. Barnard, Introductory Lectures)

S2C: Alternating Gradient Quadrupole Focusing
Electric Quadrupoles

In the axial center of a long electric quadrupole, model the fields as 2D transverse

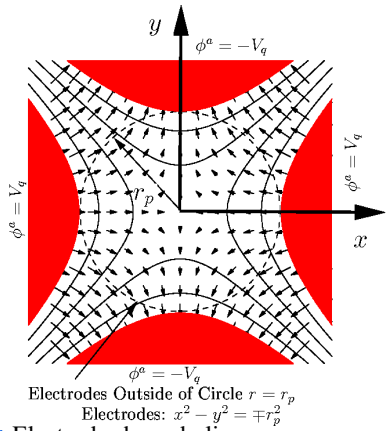

- Electrodes hyperbolic
- Structure infinitely extruded along z

2D Transverse Fields

$$\mathbf{B}^a = 0$$

$$E_x^a = -Gx$$
$$E_y^a = \quad Gy$$

$$G \equiv \frac{2V_q}{r_p^2} = -\frac{\partial E_x^a}{\partial x} = \frac{\partial E_y^a}{\partial y}$$

$= \text{Electric Gradient}$

$V_q = \text{Pole Voltage}$

$r_p = \text{Pipe Radius}$
(clear aperture)

//Aside: How can you calculate these fields?

Fields satisfy within vacuum aperture:

$$\nabla \cdot \mathbf{E}^a = 0$$
$$\nabla \times \mathbf{E}^a = 0$$
$$\Longrightarrow \qquad \mathbf{E^a} = -\nabla\phi^a$$

Choose a long axial structure with 2D hyperbolic potential surfaces:

$$\phi^a = \text{const}(x^2 - y^2)$$

Require: $\phi^a = V_q$ at $x = r_p, y = 0 \quad \Longrightarrow \quad \text{const} = V_q/r_p^2$

$$\phi^a = \frac{V_q}{r_p^2}(x^2 - y^2)$$

$$\Longrightarrow \quad E_x^a = -\frac{\partial \phi^a}{\partial x} = \frac{-2V_q}{r_p^2} x \equiv -Gx$$
$$E_y^a = -\frac{\partial \phi^a}{\partial y} = \frac{2V_q}{r_p^2} y \equiv Gy$$

$$G \equiv \frac{2V_q}{r_p^2}$$

Realistic geometries can be considerably more complicated

- Truncated hyperbolic electrodes transversely, truncated structure in z

//

Quadrupoles actually have finite axial length in z. Model this by taking the gradient G to vary in s, i.e., $G = G(s)$ with $s = z - z_{\rm center}$ (straight section)

- Variation is called the fringe-field of the focusing element
- Variation will violate the Maxwell Equations in 3D
  - Provides a reasonable first approximation in many applications
- Usually quadrupole is long, and $G(s)$ will have a flat central region and rapid variation near the ends

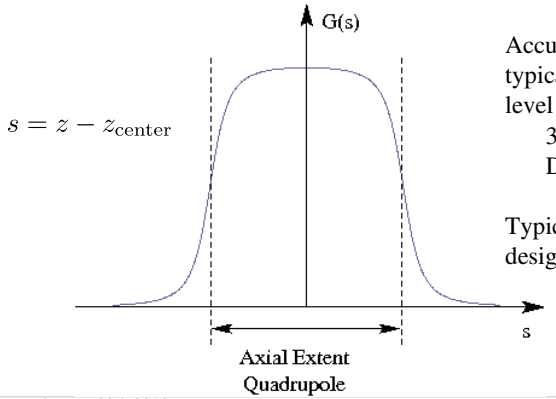

Accurate fringe calculation typically requires higher level modeling:
3D analysis
Detailed geometry

Typically employ magnetic design codes

For many applications the actual quadrupole fringe function $G(s)$ is replaced by a simpler function to allow more idealized modeling

- Replacements should be made in an "equivalent" parameter sense to be detailed later (see: lectures on Transverse Centroid and Envelope Modeling)
- Fringe functions often replaced in design studies by piecewise constant $G(s)$
  - Commonly called "hard-edge" approximation
- See S3 and Lund and Bukh, PRSTAB 7 924801 (2004), Appendix C for more details on equivalent models

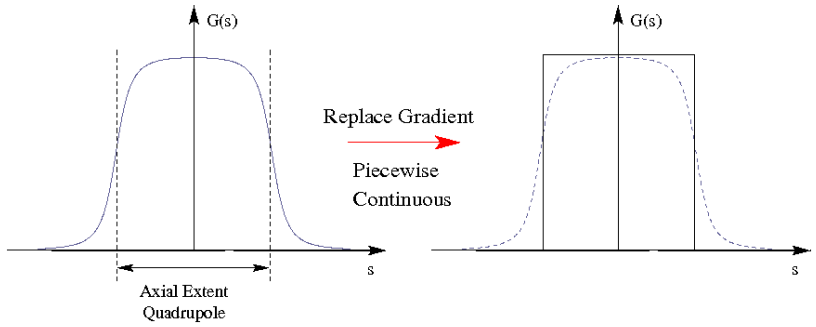

Electric quadrupole equations of motion:

- Insert applied field components into linear applied field equations and collect terms

$$x'' + \frac{(\gamma_b\beta_b)'}{(\gamma_b\beta_b)}x' + \kappa(s)x = -\frac{q}{m\gamma_b^3\beta_b^2c^2}\frac{\partial\phi}{\partial x}$$

$$y'' + \frac{(\gamma_b\beta_b)'}{(\gamma_b\beta_b)}y' - \kappa(s)y = -\frac{q}{m\gamma_b^3\beta_b^2c^2}\frac{\partial\phi}{\partial y}$$

$$\kappa(s) = \frac{qG}{m\gamma_b\beta_b^2c^2} = \frac{G}{\beta_b c[B\rho]}$$

$$G = -\frac{\partial E_x^a}{\partial x} = \frac{\partial E_y^a}{\partial y} = \frac{2V_q}{r_p^2} \qquad [B\rho] \equiv \frac{\gamma_b\beta_b mc}{q} = \text{Rigidity}$$

$$\beta_b c[B\rho] \equiv \text{Electric Rigidity}$$

- For positive/negative κ , the applied forces are Focusing/deFocusing in the x- and y-planes
- The x- and y-equations are decoupled
- Valid whether the the focusing function κ is piecewise constant or incorporates a fringe model

Simple model in limit of no acceleration ($\gamma_b\beta_b \simeq$ const) and negligible space-charge ($\phi \simeq$ const) and $\kappa =$ const:

$$\left.\begin{aligned} x'' + \kappa x &= 0 \\ y'' - \kappa y &= 0 \end{aligned}\right\} \Longrightarrow \text{orbits harmonic or hyperbolic depending on sign of } \kappa$$

General solution:

$\kappa > 0$:

$$x = x_i\cos[\sqrt{\kappa}(s-s_i)] + (x_i'/\sqrt{\kappa})\sin[\sqrt{\kappa}(s-s_i)]$$

$$x' = -\sqrt{\kappa}x_i\sin[\sqrt{\kappa}(s-s_i)] + x_i'\cos[\sqrt{\kappa}(s-s_i)]$$

$x(s_i) = x_i =$ Initial coordinate

$x'(s_i) = x_i' =$ Initial angle

$$y = y_i\cosh[\sqrt{\kappa}(s-s_i)] + (y_i'/\sqrt{\kappa})\sinh[\sqrt{\kappa}(s-s_i)]$$

$$y' = \sqrt{\kappa}y_i\sinh[\sqrt{\kappa}(s-s_i)] + y_i'\cosh[\sqrt{\kappa}(s-s_i)]$$

$y(s_i) = y_i =$ Initial coordinate

$y'(s_i) = y_i' =$ Initial angle

$\kappa < 0$:

$Exchange x and y in \kappa > 0$ case.

In terms of a transfer maps:

$\kappa > 0$:

$$\begin{bmatrix} x \\ x' \end{bmatrix}_s = \mathbf{M}_x(s|s_i) \cdot \begin{bmatrix} x \\ x' \end{bmatrix}_{s_i}$$

$$\begin{bmatrix} y \\ y' \end{bmatrix}_s = \mathbf{M}_y(s|s_i) \cdot \begin{bmatrix} y \\ y' \end{bmatrix}_{s_i}$$

$$\mathbf{M_x}(s|s_i) = \begin{bmatrix} \cos[\sqrt{\kappa}(s-s_i)] & \frac{1}{\sqrt{\kappa}}\sin[\sqrt{\kappa}(s-s_i)] \\ -\sqrt{\kappa}\sin[\sqrt{\kappa}(s-s_i)] & \cos[\sqrt{\kappa}(s-s_i)] \end{bmatrix}$$

$$\mathbf{M_y}(s|s_i) = \begin{bmatrix} \cosh[\sqrt{\kappa}(s-s_i)] & \frac{1}{\sqrt{\kappa}}\sinh[\sqrt{\kappa}(s-s_i)] \\ \sqrt{\kappa}\sinh[\sqrt{\kappa}(s-s_i)] & \cosh[\sqrt{\kappa}(s-s_i)] \end{bmatrix}$$

$\kappa < 0$:

Exchange x and y in $\kappa > 0$ case.

Quadrupoles must be arranged in a lattice where the particles traverse a sequence of optics with alternating gradient to focus strongly in both transverse directions

- Alternating gradient necessary to provide focusing in both x- and y-planes
- Alternating Gradient Focusing often abbreviated "AG" and is sometimes called "Strong Focusing"
- FODO is acronym:
  - F (Focus) in plane placed where excursions (on average) are small
  - D (deFocus) placed where excursions (on average) are large
  - O (drift) allows axial separation between elements
- Focusing lattices often (but not necessarily) periodic
  - Periodic expected to give optimal efficiency in focusing with quadrupoles
- Drifts between F and D quadrupoles allow space for: acceleration cells, beam diagnostics, vacuum pumping, ...
- Focusing strength must be limited for stability (see S5)

Example Quadrupole FODO periodic lattices with piecewise constant κ

- FODO: [Focus drift(O) DeFocus Drift(O)] has equal length drifts and same length F and D quadrupoles
- FODO is simplest possible realization of "alternating gradient" focusing
  - Can also have thin lens limit of finite axial length magnets in FODO lattice

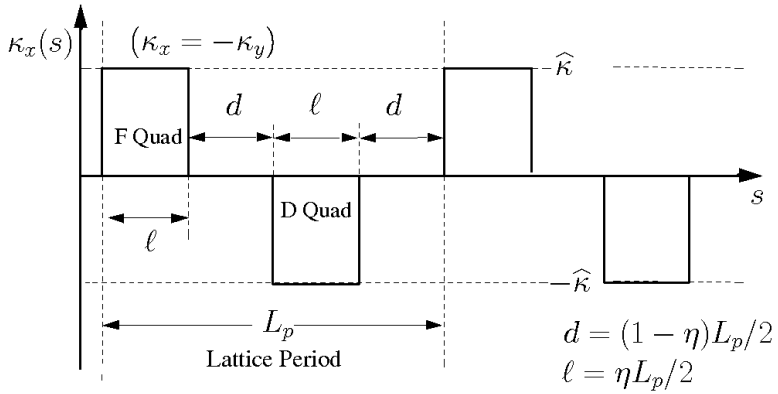

η = Occupancy $\in (0, 1]$

/// Example: Particle Orbits in a FODO Periodic Quadrupole Focusing Lattice:

Particle phase-space in x-x' with only hard-edge applied field

$L_p = 0.5$ m $\quad \kappa = \pm 50$ rad/m^2 in Quads $\quad x(0) = 1$ mm $\quad y(0) = 0$

$\eta = 0.5 \quad \phi \simeq 0 \quad \gamma_b\beta_b = \text{const} \quad x'(0) = 0 \quad y'(0) = 0$

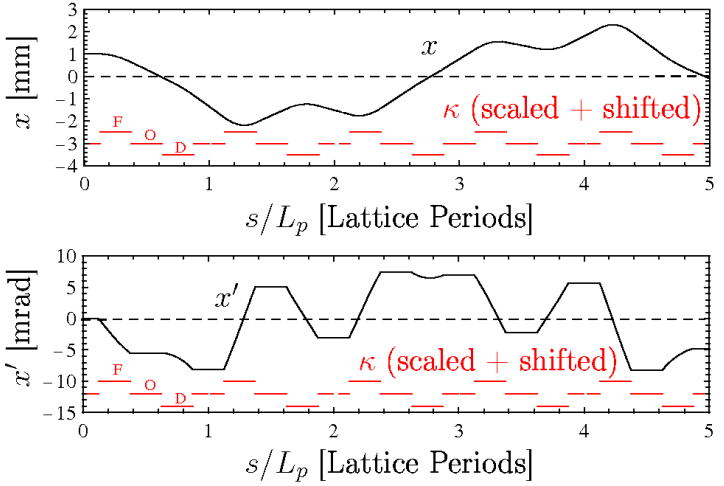

///

Comments on Orbits:

- Orbits strongly deviate from simple harmonic form due to AG focusing
  - Multiple harmonics present
- Orbit tends to be farther from axis in focusing quadrupoles and closer to axis in defocusing quadrupoles to provide net focusing
- Will find later that if the focusing is sufficiently strong, the orbit can become unstable (see: S5)
- *y*-orbit has the same properties as *x*-orbit due to the periodic structure and AG focusing
- If quadrupoles are rotated about their z-axis of symmetry, then the *x*- and *y*-equations become cross-coupled. This is called quadrupole skew coupling (see: Appendix A) and complicates the dynamics.

Some properties of particle orbits in quadrupoles with $\kappa = \text{const}$ will be analyzed in the problem sets

S2D: Alternating Gradient Quadrupole Focusing
Magnetic Quadrupoles

In the axial center of a long magnetic quadrupole, model fields as 2D transverse

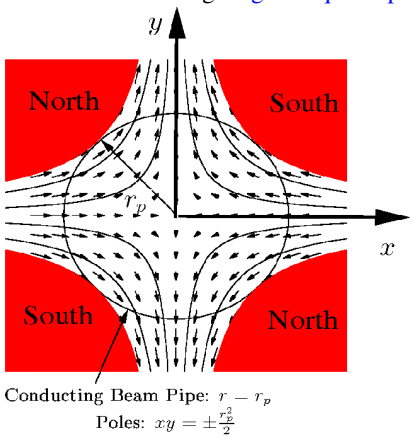

- Magnetic (ideal iron) poles hyperbolic
- Structure infinitely extruded along *z*

2D Transverse Fields

$$\mathbf{E}_\perp^a = 0$$

$$B_x^a = Gy$$
$$B_y^a = Gx$$
$$B_z^a = 0$$

$$G \equiv \frac{B_q}{r_p} = \frac{\partial B_x^a}{\partial y} = \frac{\partial B_y^a}{\partial x}$$
$$= \text{Magnetic Gradient}$$

$$B_q = |\mathbf{B}^a|_{r=r_p} = \text{Pole Field}$$
$$r_p = \text{Pipe Radius}$$

//Aside: How can you calculate these fields?

Fields satisfy within vacuum aperture:

$$\nabla \cdot \mathbf{B}^a = 0$$
$$\nabla \times \mathbf{B}^a = 0 \quad \Longrightarrow \quad \mathbf{B^a} = -\nabla\phi^a$$

Analogous to electric case, BUT magnetic force is different so rotate potential surfaces by 45 degrees:

Electric

$$\mathbf{F}_\perp = -q\frac{\partial \phi^a}{\partial \mathbf{x}_\perp}$$

$$\phi^a = \text{const}(x^2 - y^2)$$

Magnetic

$$\mathbf{F}_\perp = -q\beta_b c\hat{\mathbf{z}} \times \frac{\partial \phi^a}{\partial \mathbf{x}_\perp}$$

expect electric potential form rotated by 45 degrees ...

$$x \to \frac{1}{\sqrt{2}}x - \frac{1}{\sqrt{2}}y$$
$$y \to \frac{1}{\sqrt{2}}x + \frac{1}{\sqrt{2}}y$$

$$\phi^a \to \phi^a = -\text{const} \cdot xy$$

$$\Longrightarrow \quad B_x^a = -\frac{\partial \phi^a}{\partial x} = \text{const} \cdot y$$
$$B_y^a = -\frac{\partial \phi^a}{\partial y} = \text{const} \cdot x$$

Require: $|\mathbf{B}^a| = B_p$ at $r = \sqrt{x^2 + y^2} = r_p \quad \Longrightarrow \quad \text{const} = B_p/r_p$

$$\Longrightarrow \phi^a = -\frac{B_p}{r_p}xy \qquad G = \frac{B_p}{r_p}$$

Realistic geometries can be considerably more complicated

- Truncated hyperbolic poles, truncated structure in *z*
- Both effects give nonlinear focusing terms

//

Analogously to the electric quadrupole case, take $G = G(s)$

- Same comments made on electric quadrupole fringe in S2C are directly applicable to magnetic quadrupoles

Magnetic quadrupole equations of motion:

- Insert field components into linear applied field equations and collect terms

$$x'' + \frac{(\gamma_b\beta_b)'}{(\gamma_b\beta_b)}x' + \kappa(s)x = -\frac{q}{m\gamma_b^3\beta_b^2c^2}\frac{\partial\phi}{\partial x}$$

$$y'' + \frac{(\gamma_b\beta_b)'}{(\gamma_b\beta_b)}y' - \kappa(s)y = -\frac{q}{m\gamma_b^3\beta_b^2c^2}\frac{\partial\phi}{\partial y}$$

$$\kappa(s) = \frac{qG}{m\gamma_b\beta_bc} = \frac{G}{[B\rho]}$$

$$G = \frac{\partial B_x^a}{\partial y} = \frac{\partial B_y^a}{\partial x} = \frac{B_q}{r_p} \qquad [B\rho] \equiv \frac{\gamma_b\beta_bmc}{q} = \text{Rigidity}$$

- Equations identical to the electric quadrupole case in terms of $\kappa(s)$
- All comments made on electric quadrupole focusing lattice are immediately applicable to magnetic quadruples: just apply different κ definitions in design
- Scaling of κ with energy different than electric case impacts applicability

$$\kappa = \begin{cases} \frac{G}{\beta_bc[B\rho]} & \text{Electric Focusing;} \quad G = \frac{\partial E_y^a}{\partial y} = \frac{2V_q}{r_p^2} \\ \frac{G}{[B\rho]} & \text{Magnetic Focusing;} \quad G = \frac{\partial B_x^a}{\partial y} = \frac{B_q}{r_p} \end{cases}$$

- Electric focusing weaker for higher particle energy (larger β_b)
- Technical limit values of gradients
  - Voltage holding for electric
  - Material properties (iron saturation, superconductor limits, ...) for magnetic
- See JJB Intro lectures for discussion on focusing technology choices

Different energy dependence also gives different dispersive properties when beam has axial momentum spread:

$$\delta \equiv \frac{\delta p}{p_0} = \text{Fractional Momentum Error}$$

$$\kappa \to \begin{cases} \frac{\kappa}{(1+\delta)^2} & \text{Electric Focusing} \\ \frac{\kappa}{1+\delta} & \text{Magnetic Focusing} \end{cases}$$

- Electric case further complicated because δ couples to the transverse motion since particles crossing higher electrostatic potentials are accelerated/deaccelerated

S2E: Solenoidal Focusing

The field of an ideal magnetic solenoid is invariant under transverse rotations about it's axis of symmetry (z) can be expanded in terms of the on-axis field as:

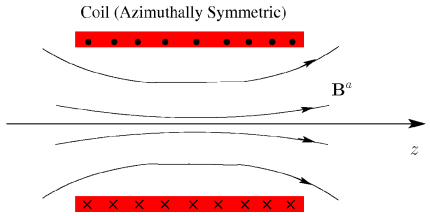

Vacuum Maxwell equations:

$$\nabla \cdot \mathbf{B}^a = 0$$
$$\nabla \times \mathbf{B}^a = 0$$

Imply $\mathbf{B}^a$ can be expressed in terms of on-axis field $\mathbf{B}_z^a(r=0,z)$

$$\mathbf{E}^a = 0$$

$$\mathbf{B}_\perp^a = \frac{1}{2}\sum_{\nu=1}^{\infty}\frac{(-1)^\nu}{\nu!(\nu-1)!}\frac{\partial^{2\nu-1}B_{z0}(z)}{\partial z^{2\nu-1}}\left(\frac{|\mathbf{x}_\perp|}{2}\right)^{2\nu-2}\mathbf{x}_\perp$$

$$B_z^a = B_{z0}(z) + \sum_{\nu=1}^{\infty}\frac{(-1)^\nu}{(\nu!)^2}\frac{\partial^{2\nu}B_{z0}(z)}{\partial z^{2\nu}}\left(\frac{|\mathbf{x}_\perp|}{2}\right)^{2\nu}$$

$$B_{z0}(z) \equiv B_z^a(\mathbf{x}_\perp = 0, z) = \text{On-Axis Field}$$

See Appendix D or Reiser, *Theory and Design of Charged Particle Beams*, Sec. 3.3.1

Writing out explicitly the terms of this expansion:

$$\mathbf{B}^a(r,z) = \hat{\mathbf{r}}B_r^a(r,z) + \hat{\mathbf{z}}B_z^a(r,z) \qquad r = \sqrt{x^2+y^2}$$
$$= (-\hat{\mathbf{x}}\sin\theta + \hat{\mathbf{y}}\cos\theta)B_r^a(r,z) + \hat{\mathbf{z}}B_z^a(r,z)$$

where

$$B_r^a(r,z) = \sum_{\nu=1}^{\infty}\frac{(-1)^\nu}{\nu!(\nu-1)!}B_{z0}^{(2\nu-1)}(z)\left(\frac{r}{2}\right)^{2\nu-1}$$
$$= \boxed{-\frac{B_{z0}'(z)}{2}r} + \frac{B_{z0}^{(3)}(z)}{16}r^3 - \frac{B_{z0}^{(5)}(z)}{384}r^5 + \frac{B_{z0}^{(7)}(z)}{18432}r^7 - \frac{B_{z0}^{(9)}(z)}{1474560}r^9 + \ldots$$

$$B_z^a(r,z) = \sum_{\nu=0}^{\infty}\frac{(-1)^\nu}{(\nu!)^2}B_{z0}^{(2\nu)}(z)\left(\frac{r}{2}\right)^{2\nu}$$
$$= \boxed{B_{z0}(z)} - \frac{B_{z0}''(z)}{4}r^2 + \frac{B_{z0}^{(4)}(z)}{64}r^4 - \frac{B_{z0}^{(6)}(z)}{2304}r^6 + \frac{B_{z0}^{(8)}(z)}{147456}r^8 + \ldots$$

$\boxed{\cdots}$ Linear Terms

$$B_{z0}(z) \equiv B_z^a(r=0,z) = \text{On-axis Field}$$

$$B_{z0}^{(n)}(z) \equiv \frac{\partial^n B_{z0}(z)}{\partial z^n} \qquad B_{z0}'(z) \equiv \frac{\partial B_{z0}(z)}{\partial z} \qquad B_{z0}''(z) \equiv \frac{\partial^2 B_{z0}(z)}{\partial z^2}$$

For modeling, we truncate the expansion using only leading-order terms to obtain:

- Corresponds to linear dynamics in the equations of motion

$$B_x^a = -\frac{1}{2}\frac{\partial B_{z0}(z)}{\partial z}x$$
$$B_y^a = -\frac{1}{2}\frac{\partial B_{z0}(z)}{\partial z}y \qquad B_{z0}(z) \equiv B_z^a(\mathbf{x}_\perp = 0, z)$$
$$B_z^a = B_{z0}(z) \qquad = \text{On-Axis Field}$$

Note that this truncated expansion is divergence free:

$$\nabla \cdot \mathbf{B}^a = -\frac{1}{2}\frac{\partial B_{z0}}{\partial z}\frac{\partial}{\partial \mathbf{x}_\perp}\cdot\mathbf{x}_\perp + \frac{\partial}{\partial z}B_{z0} \quad = 0$$

but not curl free within the vacuum aperture:

$$\nabla \times \mathbf{B}^a = \frac{1}{2}\frac{\partial^2 B_{z0}(z)}{\partial z^2}(-\hat{\mathbf{x}}y + \hat{\mathbf{y}}x)$$
$$= \frac{1}{2}\frac{\partial^2 B_{z0}(z)}{\partial z^2}r(-\hat{\mathbf{x}}\sin\theta + \hat{\mathbf{y}}\cos\theta) = \frac{1}{2}\frac{\partial^2 B_{z0}(z)}{\partial z^2}r\hat{\theta}$$

- Nonlinear terms needed to satisfy 3D Maxwell equations

Solenoid equations of motion:

- Insert field components into equations of motion and collect terms

$$x'' + \frac{(\gamma_b\beta_b)'}{(\gamma_b\beta_b)}x' - \frac{B'_{z0}(s)}{2[B\rho]}y - \frac{B_{z0}(s)}{[B\rho]}y' = -\frac{q}{m\gamma_b^3\beta_b^2c^2}\frac{\partial\phi}{\partial x}$$
$$y'' + \frac{(\gamma_b\beta_b)'}{(\gamma_b\beta_b)}y' + \frac{B'_{z0}(s)}{2[B\rho]}x + \frac{B_{z0}(s)}{[B\rho]}x' = -\frac{q}{m\gamma_b^3\beta_b^2c^2}\frac{\partial\phi}{\partial y}$$

$$[B\rho] \equiv \frac{\gamma_b\beta_b mc}{q} = \text{Rigidity} \qquad \frac{B_{z0}(s)}{[B\rho]} = \frac{\omega_c(s)}{\gamma_b\beta_b c}$$

$$\omega_c(s) = \frac{qB_{z0}(s)}{m} = \text{Cyclotron Frequency (in applied axial magnetic field)}$$

- Equations are linearly cross-coupled in the applied field terms
  - x equation depends on y, y'
  - y equation depends on x, x'

It can be shown (see: Appendix B) that the linear cross-coupling in the applied field can be removed by an s-varying transformation to a rotating "Larmor" frame:

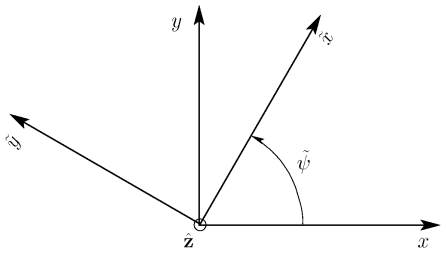

$\tilde{\ldots}$ used to denote rotating frame variables

$$\tilde{x} = \quad x\cos\tilde{\psi}(s) + y\sin\tilde{\psi}(s)$$
$$\tilde{y} = -x\sin\tilde{\psi}(s) + y\cos\tilde{\psi}(s)$$

$$\tilde{\psi}(s) = -\int_{s_i}^{s} d\bar{s}\; k_L(\bar{s})$$

$$k_L(s) \equiv \frac{B_{z0}(s)}{2[B\rho]} = \frac{\omega_c(s)}{2\gamma_b\beta_b c}$$
$$= \text{Larmor wave number}$$

$s = s_i$ defines initial condition

If the beam space-charge is *axisymmetric*:

$$\frac{\partial\phi}{\partial\mathbf{x}_\perp} = \frac{\partial\phi}{\partial r}\frac{\partial r}{\partial\mathbf{x}_\perp} = \frac{\partial\phi}{\partial r}\frac{\mathbf{x}_\perp}{r}$$

then the space-charge term also decouples under the Larmor transformation and the equations of motion can be expressed in fully uncoupled form:

$$\tilde{x}'' + \frac{(\gamma_b\beta_b)'}{(\gamma_b\beta_b)}\tilde{x}' + \kappa(s)\tilde{x} = -\frac{q}{m\gamma_b^3\beta_b^2c^2}\frac{\partial\phi}{\partial r}\frac{\tilde{x}}{r}$$
$$\tilde{y}'' + \frac{(\gamma_b\beta_b)'}{(\gamma_b\beta_b)}\tilde{y}' + \kappa(s)\tilde{y} = -\frac{q}{m\gamma_b^3\beta_b^2c^2}\frac{\partial\phi}{\partial r}\frac{\tilde{y}}{r}$$

$$\kappa(s) = k_L^2(s) \equiv \left[\frac{B_{z0}(s)}{2[B\rho]}\right]^2 = \left[\frac{\omega_c(s)}{2\gamma_b\beta_b c}\right]^2$$

Will demonstrate this in problems for the simple case of: $B_{z0}(s) = \text{const}$

- Because Larmor frame equations are in the same form as continuous and quadrupole focusing with a different κ, for solenoidal focusing we implicitly work in the Larmor frame and simplify notation by dropping the tildes:

$$\tilde{\mathbf{x}}_\perp \to \mathbf{x}_\perp$$

/// Aside: Notation:

A common theme of this class will be to introduce new effects and generalizations while keeping formulations looking as similar as possible to the the most simple representations given. When doing so, we will often use "tildes" to denote transformed variables to stress that the new coordinates have, in fact, a more complicated form that must be interpreted in the context of the analysis being carried out. Some examples:

- Larmor frame transformations for Solenoidal focusing
  See: Appendix B
- Normalized variables for analysis of accelerating systems
  See: S10
- Coordinates expressed relative to the beam centroid
  See: S.M. Lund, lectures on Transverse Centroid and Envelope Model
- Variables used to analyze Einzel lenses
  See: J.J. Barnard, Introductory Lectures

///

Solenoid periodic lattices can be formed similarly to the quadrupole case

- Drifts placed between solenoids of finite axial length
  - Allows space for diagnostics, pumping, acceleration cells, etc.
- Analogous equivalence cases to quadrupole
  - Piecewise constant κ often used
- Fringe can be more important for solenoids

Simple hard-edge solenoid lattice with piecewise constant κ

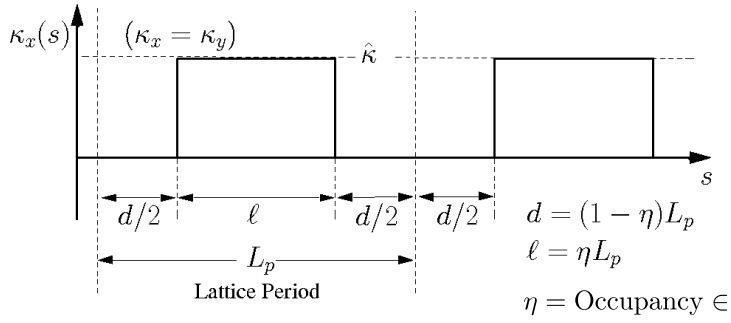

/// Example: Larmor Frame Particle Orbits in a Periodic Solenoidal Focusing Lattice: $\tilde{x} - \tilde{x}'$ phase-space for hard edge elements and applied fields

$L_p = 0.5$ m $\quad \kappa = 20$ rad/m^2 in Solenoids $\quad \tilde{x}(0) = 1$ mm $\quad \tilde{y}(0) = 0$

$\eta = 0.5 \quad \phi \simeq 0 \quad \gamma_b\beta_b = \text{const} \quad \tilde{x}'(0) = 0 \quad \tilde{y}'(0) = 0$

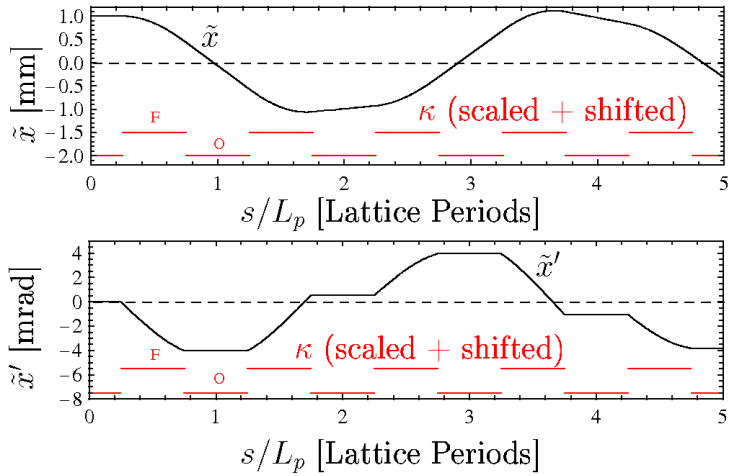

Contrast of Larmor-Frame and Lab-Frame Orbits

- Same initial condition

Larmor-Frame Coordinate Orbit in transformed x-plane only

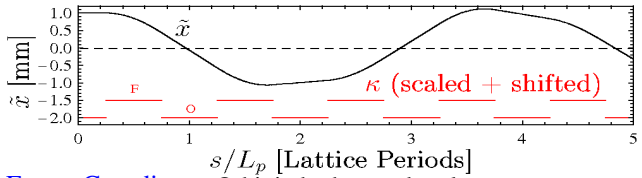

Lab-Frame Coordinate Orbit in both x- and y-planes

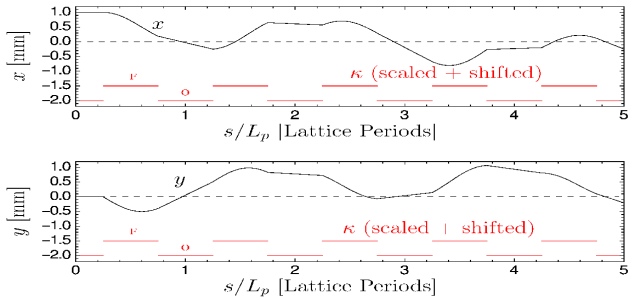

Calculate using transfer matrices in Appendix C

Contrast of Larmor-Frame and Lab-Frame Orbits

- Same initial condition

Larmor-Frame Angle

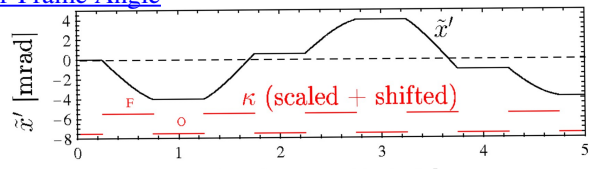

Lab-Frame Angle

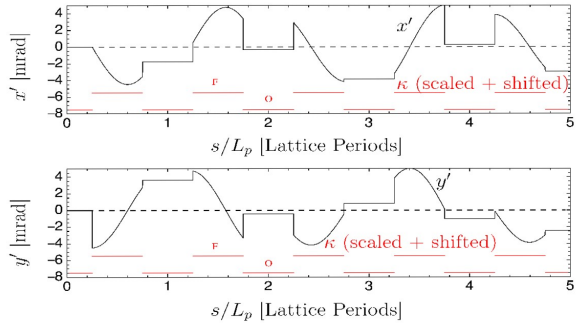

Calculate using transfer matrices in Appendix C

Additional perspectives of particle orbit in solenoid transport channel

- Same initial condition

Radius evolution (Lab or Larmor Frame: radius same)

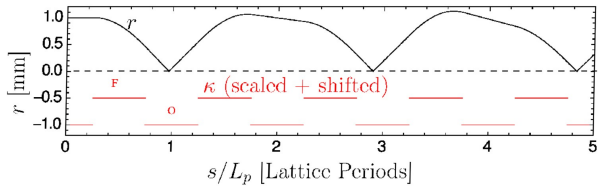

Side- (2 view points) and End-View Projections of 3D Lab-Frame Orbit

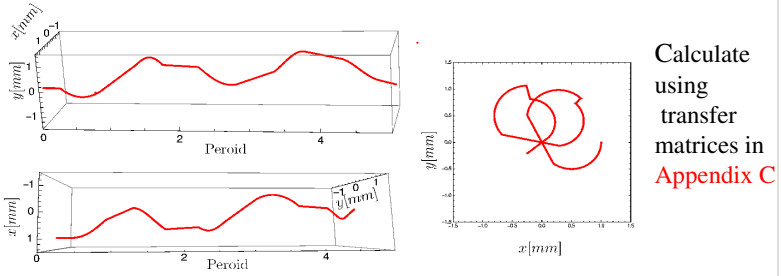

Calculate using transfer matrices in Appendix C

Larmor angle and angular momentum of particle orbit in solenoid transport channel

- Same initial condition

Larmor Angle

$$\tilde{\psi}(s) = -\int_{s_i}^{s} d\bar{s}\; k_L(\bar{s}) \qquad k_L(s) \equiv \frac{B_{z0}(s)}{2[B\rho]}$$

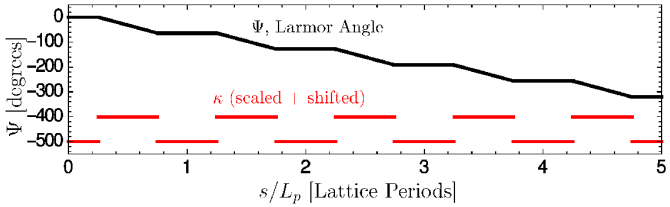

Angular Momentum and Canonical Angular Momentum (see Sec. S2G)

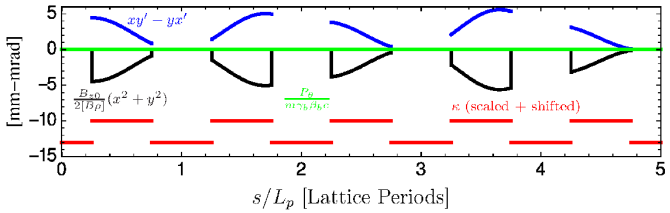

///

Comments on Orbits:

- See Appendix C for details on calculation
  - Discontinuous fringe of hard-edge model must be treated carefully if integrating in the laboratory-frame.
- Larmor-frame orbits strongly deviate from simple harmonic form due to periodic focusing
  - Multiple harmonics present
  - Less complicated than quadrupole AG focusing case when interpreted in the Larmor frame due to the optic being focusing in both planes
- Orbits transformed back into the Laboratory frame using Larmor transform (see: Appendix B and Appendix C)
  - Laboratory frame orbit exhibits more complicated *x*-*y* plane coupled oscillatory structure
- Will find later that if the focusing is sufficiently strong, the orbit can become unstable (see: S5)
- Larmor frame *y*-orbits have same properties as the *x*-orbits due to the equations being decoupled and identical in form in each plane
  - In example, Larmor *y*-orbit is zero due to simple initial condition in *x*-plane
  - Lab *y*-orbit is nozero due to *x*-*y* coupling

Comments on Orbits (continued):

- Larmor angle advances continuously even for hard-edge focusing
- Mechanical angular momentum jumps discontinuously going into and out of the solenoid
  - Particle spins up and down going into and out of the solenoid
  - No mechanical angular momentum outside of solenoid due to the choice of intial condition in this example (initial x-plane motion)
- Canonical angular momentum P_θ is conserved in the 3D orbit evolution
  - As expected from analysis in S2G
  - Invariance provides a good check on dynamics
  - P_θ in example has zero value due to the specific (x-plane) choice of initial condition. Other choices can give nonzero values and finite mechanical angular momentum in drifts.

Some properties of particle orbits in solenoids with piecewise $\kappa = \text{const}$ will be analyzed in the problem sets

///

S2F: Summary of Transverse Particle Equations of Motion

In linear applied focusing channels, without momentum spread or radiation, the particle equations of motion in both the x- and y-planes expressed as:

$$x'' + \frac{(\gamma_b\beta_b)'}{(\gamma_b\beta_b)}x' + \kappa_x(s)x = -\frac{q}{m\gamma_b^3\beta_b^2c^2}\frac{\partial}{\partial x}\phi$$

$$y'' + \frac{(\gamma_b\beta_b)'}{(\gamma_b\beta_b)}y' + \kappa_y(s)y = -\frac{q}{m\gamma_b^3\beta_b^2c^2}\frac{\partial}{\partial y}\phi$$

$\kappa_x(s) = x$-focusing function of lattice

$\kappa_y(s) = y$-focusing function of lattice

Common focusing functions:

Continuous:
$$\kappa_x(s) = \kappa_y(s) = k_{\beta 0}^2 = \text{const}$$

Quadrupole (Electric or Magnetic):
$$\kappa_x(s) = -\kappa_y(s) = \kappa(s)$$

Solenoidal (equations must be interpreted in Larmor Frame: see Appendix B):
$$\kappa_x(s) = \kappa_y(s) = \kappa(s)$$

Although the equations have the same form, the couplings to the fields are different which leads to different regimes of applicability for the various focusing technologies with their associated technology limits:

Focusing:

Continuous:
$$\kappa_x(s) = \kappa_y(s) = k_{\beta 0}^2 = \text{const}$$
Good qualitative guide (see later material/lecture)
BUT not physically realizable (see S2B)

Quadrupole:
$$\kappa_x(s) = -\kappa_y(s) = \begin{cases} \frac{G(s)}{\beta_b c[B\rho]}, & \text{Electric} \\ \frac{G(s)}{c[B\rho]}, & \text{Magnetic} \end{cases} \qquad [B\rho] = \frac{m\gamma_b\beta_b c}{q}$$

G is the field gradient which for linear applied fields is:
$$G(s) = \begin{cases} -\frac{\partial E_x^a}{\partial x} = \frac{\partial E_y^a}{\partial y} = \frac{2V_q}{r_p^2}, & \text{Electric} \\ \frac{\partial B_x^a}{\partial y} = \frac{\partial B_y^a}{\partial x} = \frac{B_p}{r_p}, & \text{Magnetic} \end{cases}$$

Solenoid:
$$\kappa_x(s) = \kappa_y(s) = k_L^2(s) = \left[\frac{B_{z0}(s)}{2[B\rho]}\right]^2 = \left[\frac{\omega_c(s)}{2\gamma_b\beta_b c}\right]^2 \qquad \omega_c(s) = \frac{qB_{z0}(s)}{m}$$

It is instructive to review the structure of solutions of the transverse particle equations of motion in the absence of:

Space-charge: $\frac{\partial\phi}{\partial x} \sim \frac{\partial\phi}{\partial y} \sim 0$

Acceleration: $\gamma_b\beta_b \simeq \text{const} \quad \Longrightarrow \frac{(\gamma_b\beta_b)'}{(\gamma_b\beta_b)} \simeq 0$

In this simple limit, the x and y-equations are of the same Hill's Equation form:

$$x'' + \kappa_x(s)x = 0$$
$$y'' + \kappa_y(s)y = 0$$

- These equations are central to transverse dynamics in conventional accelerator physics (weak space-charge and acceleration)
  - Will study how solutions change with space-charge in later lectures

In many cases beam transport lattices are designed where the applied focusing functions are periodic:

$$\kappa_x(s + L_p) = \kappa_x(s)$$
$$\kappa_y(s + L_p) = \kappa_y(s) \qquad L_p = \text{Lattice Period}$$

Common, simple examples of periodic lattices:

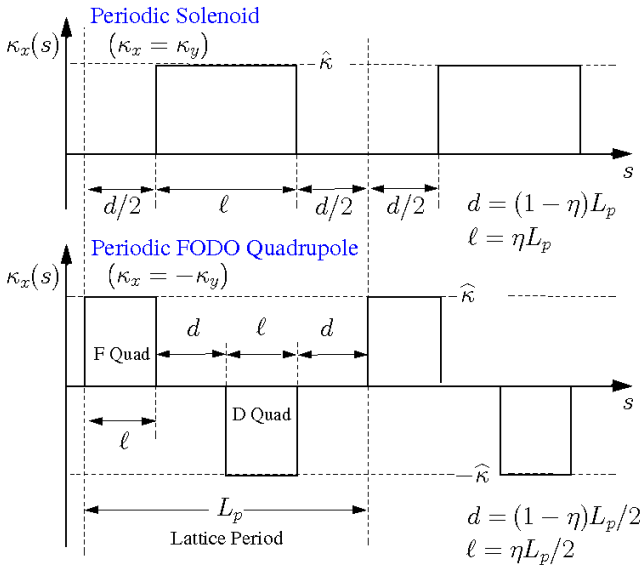

However, the focusing functions need not be periodic:

- Often take periodic or continuous in this class for simplicity of interpretation

Focusing functions can vary strongly in many common situations:

- Matching and transition sections
- Strong acceleration
- Significantly different elements can occur within periods of lattices in rings
  - "Panofsky" type (wide aperture along one plane) quadrupoles for beam insertion and extraction in a ring

Example of Non-Periodic Focusing Functions: Beam Matching Section

Maintains alternating-gradient structure but not quasi-periodic

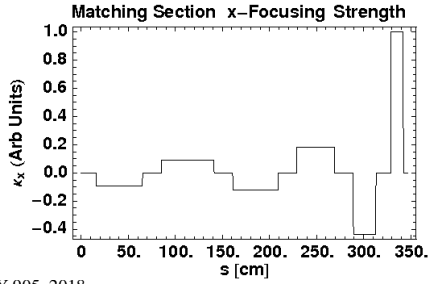

Example corresponds to High Current Experiment Matching Section (hard edge equivalent) at LBNL (2002)

Equations presented in this section apply to a single particle moving in a beam under the action of linear applied focusing forces. In the remaining sections, we will (mostly) neglect space-charge ($\phi \to 0$) as is conventional in the standard theory of low-intensity accelerators.

- What we learn from treatment will later aid analysis of space-charge effects
  - Appropriate variable substitutions will be made to apply results
- Important to understand basic applied field dynamics since space-charge complicates
  - Results in plasma-like collective response

/// Example: We will see in Transverse Centroid and Envelope Descriptions of Beam Evolution that the linear particle equations of motion can be applied to analyze the evolution of a beam when image charges are neglected

$$x \to x_c \equiv \langle x \rangle_\perp \quad x - \text{centroid}$$
$$y \to y_c \equiv \langle y \rangle_\perp \quad y - \text{centroid}$$

///

S2G: Conservation of Angular Momentum in Axisymmetric Focusing Systems

Background:

Goal: find an invariant for axisymmetric focusing systems which can help us further interpret/understand the dynamics.

In Hamiltonian descriptions of beam dynamics one must employ proper canonical conjugate variables such as (x-plane):

$$\begin{aligned} x &= && \text{Canonical Coordinate} \\ P_x &= p_x + qA_x = && \text{Canonical Momentum} \end{aligned}$$

+ analogous y-plane

Here, $\boldsymbol{A}$ denotes the vector potential of the (static for cases of field models considered here) applied magnetic field with:

$$\mathbf{B}^a = \nabla \times \mathbf{A}$$

For the cases of linear applied magnetic fields in this section, we have:

$$\mathbf{A} = \begin{cases} \hat{\mathbf{z}}\frac{G}{2}(y^2 - x^2), & \text{Magnetic Quadrupole Focusing} \\ -\hat{\mathbf{x}}\frac{1}{2}B_{z0}y + \hat{\mathbf{y}}\frac{1}{2}B_{z0}x, & \text{Solenoidal Focusing} \\ 0, & \text{Otherwise} \end{cases}$$

For continuous, electric or magnetic quadrupole focusing without acceleration ($\gamma_b\beta_b = \text{const}$) , it is straightforward to verify that *x,x′* and *y,y′* are canonical coordinates and that the correct equations of motion are generated by the Hamiltonian:

$$H_\perp = \frac{1}{2}x'^2 + \frac{1}{2}y'^2 + \frac{1}{2}\kappa_x x^2 + \frac{1}{2}\kappa_y y^2 + \frac{q\phi}{m\gamma_b^3\beta_b^2c^3}$$

$$\frac{d}{ds}x = \frac{\partial H_\perp}{\partial x'} \qquad \frac{d}{ds}x = \frac{\partial H_\perp}{\partial y'}$$

$$\frac{d}{ds}x' = -\frac{\partial H_\perp}{\partial x} \qquad \frac{d}{ds}y' = -\frac{\partial H_\perp}{\partial y}$$

Giving the familiar equations of motion:

$$x'' + \kappa_x x = -\frac{q}{m\gamma_b^3\beta_b^2c^2}\frac{\partial\phi}{\partial x}$$

$$y'' + \kappa_y y = -\frac{q}{m\gamma_b^3\beta_b^2c^2}\frac{\partial\phi}{\partial y}$$

For solenoidal magnetic focusing without acceleration, it can be verified that we can take (tilde) canonical variables:

- Tildes *do not* denote Larmor transform variables here !

$$\tilde{x} = x \qquad \tilde{y} = y$$

$$\tilde{x}' = x' - \frac{B_{z0}}{2[B\rho]}y \qquad \tilde{y}' = y' + \frac{B_{z0}}{2[B\rho]}x \qquad [B\rho] \equiv \frac{m\gamma_b\beta_b c}{q}$$

With Hamiltonian:

$$\tilde{H}_\perp = \frac{1}{2}\left[\left(\tilde{x}' + \frac{B_{z0}}{2[B\rho]}\tilde{y}\right)^2 + \left(\tilde{y}' - \frac{B_{z0}}{2[B\rho]}\tilde{x}\right)^2\right] + \frac{q\phi}{m\gamma_b^3\beta_b^2c^3}$$

$$\frac{d}{ds}\tilde{x} = \frac{\partial\tilde{H}_\perp}{\partial\tilde{x}'} \qquad \frac{d}{ds}\tilde{y} = \frac{\partial\tilde{H}_\perp}{\partial\tilde{y}'}$$

$$\frac{d}{ds}\tilde{x}' = -\frac{\partial H_\perp}{\partial\tilde{x}} \qquad \frac{d}{ds}\tilde{y}' = -\frac{\partial H_\perp}{\partial\tilde{y}}$$

Caution: Primes do not mean *d/ds* in tilde variables here: just notation to distinguish "momentum" variable!

Giving (after some algebra) the familiar equations of motion:

$$x'' - \frac{B'_{z0}(s)}{2[B\rho]}y - \frac{B_{z0}(s)}{[B\rho]}y' = -\frac{q}{m\gamma_b^3\beta_b^2c^2}\frac{\partial\phi}{\partial x}$$

$$y'' + \frac{B'_{z0}(s)}{2[B\rho]}x + \frac{B_{z0}(s)}{[B\rho]}x' = -\frac{q}{m\gamma_b^3\beta_b^2c^2}\frac{\partial\phi}{\partial y}$$

Canonical angular momentum

One expects from general considerations (Noether's Theorem in dynamics) that systems with a symmetry have a conservation constraint associated with the generator of the symmetry. So for systems with azimuthal symmetry ($\partial/\partial\theta = 0$), one expects there to be a conserved canonical angular momentum (generator of rotations). Based on the Hamiltonian dynamics structure, examine:

$$P_\theta \equiv [\mathbf{x}\times\mathbf{P}]\cdot\hat{\mathbf{z}} = [\mathbf{x}\times(\mathbf{p}+q\mathbf{A})]\cdot\hat{\mathbf{z}}$$

This is exactly equivalent to

- Here γ factor is exact (*not* paraxial)

$$P_\theta = (xp_y - yp_x) + q(xA_y - yA_x)$$
$$= r(p_\theta + qA_\theta) = m\gamma r^2\dot{\theta} + qrA_\theta$$

Or employing the usual paraxial approximation steps:

$$P_\theta \simeq m\gamma_b\beta_b c(xy' - yx') + q(xA_y - yA_x)$$
$$= m\gamma_b\beta_b cr^2\theta' + qrA_\theta$$

Inserting the vector potential components consistent with linear approximation solenoid focusing in the paraxial expression gives:

- Applies to (superimposed or separately) to continuous, magnetic or electric quadrupole, or solenoidal focusing since $A_\theta \neq 0$ only for solenoidal focusing

$$P_\theta \simeq m\gamma_b\beta_b c(xy' - yx') + \frac{qB_{z0}}{2}(x^2+y^2)$$
$$= m\gamma_b\beta_b cr^2\theta' + \frac{qB_{z0}}{2}r^2$$

For a coasting beam ($\gamma_b\beta_b = \text{const}$), it is often convenient to analyze:

- Later we will find this is analogous to use of "unnormalized" variables used in calculation of ordinary emittance rather than normalized emittance

$$\frac{P_\theta}{m\gamma_b\beta_b c} = xy' - yx' + \frac{B_{z0}}{2[B\rho]}(x^2+y^2) \qquad [B\rho] \equiv \frac{m\gamma_b\beta_b c}{q}$$
$$= r^2\theta' + \frac{B_{z0}}{2[B\rho]}r^2$$

Conservation of canonical angular momentum

To investigate situations where the canonical angular momentum is a constant of the motion for a beam evolving in linear applied fields, we differentiate P_θ with respect to s and apply equations of motion

Equations of Motion:

Including acceleration effects again, we summarize the equations of motion as:

- Applies to continuous, quadrupole (electric + magnetic), and solenoid focusing as expressed
- Several types of focusing can also be superimposed
  - Show for superimposed solenoid

$$x'' + \frac{(\gamma_b\beta_b)'}{(\gamma_b\beta_b)}x' + \kappa_x x - \frac{B'_{z0}(s)}{2[B\rho]}y - \frac{B_{z0}(s)}{[B\rho]}y' = -\frac{q}{m\gamma_b^3\beta_b^2c^2}\frac{\partial\phi}{\partial x}$$

$$y'' + \frac{(\gamma_b\beta_b)'}{(\gamma_b\beta_b)}y' + \kappa_y y + \frac{B'_{z0}(s)}{2[B\rho]}x + \frac{B_{z0}(s)}{[B\rho]}x' = -\frac{q}{m\gamma_b^3\beta_b^2c^2}\frac{\partial\phi}{\partial y}$$

$$[B\rho] = \frac{m\gamma_b\beta_b c}{q} \qquad \kappa_x(s) = \begin{cases} k_{\beta 0}^2 = \text{const}, & \text{Continuous Focus } (\kappa_y = \kappa_x) \\ \frac{G(s)}{\beta_b c[B\rho]}, & \text{Electric Quadrupole Focus } (\kappa_y = -\kappa_x) \\ \frac{G(s)}{c[B\rho]}, & \text{Magnetic Quadrupole Focus } (\kappa_y = -\kappa_x) \end{cases}$$

Employ the paraxial form of P_θ consistent with the possible existence of a solenoid magnetic field:

- Formula also applies as expressed to continuous and quadrupole focusing

$$\mathrm{P}_\theta = m\gamma_b\beta_b c(xy' - yx') + \tfrac{qB_{z0}}{2}(x^2 + y^2)$$

Differentiate and apply equations of motion:

- Intermediate algebraic steps not shown

$$\frac{d}{ds}P_\theta = mc(\gamma_b\beta_b)'(xy' - yx') + mc(\gamma_b\beta_b)(xy'' - yx'')$$
$$+ \frac{qB'_{z0}}{2}(x^2 + y^2) + qB_{z0}(xx' + yy')$$
$$= mc(\gamma_b\beta_b)[\kappa_x - \kappa_y]xy - \frac{q}{\gamma_b^2\beta_b c}\left(x\frac{\partial\phi}{\partial y} - y\frac{\partial\phi}{\partial x}\right)$$

So *IF*:

1) $\kappa_x = \kappa_y$
   - Valid continuous or solenoid focusing
   - Invalid for quadrupole focusing

2) $x\frac{\partial\phi}{\partial y} - y\frac{\partial\phi}{\partial x} = \frac{\partial\phi}{\partial\theta} = 0$
   - Axisymmetric beam

$$\frac{d}{ds}P_\theta = 0 \qquad \Longrightarrow \qquad P_\theta = \text{const}$$

For:

- Continuous focusing
- Linear optics solenoid magnetic focusing
- Other axisymmetric electric optics not covered such as Einzel lenses …

$$\mathrm{P}_\theta = m\gamma_b\beta_b c(xy' - yx') + \tfrac{qB_{z0}}{2}(x^2 + y^2) = \text{const}$$

$$m\gamma_b\beta_b c(xy' - yx') = \text{Mechanical Angular Momentum Term}$$

$$\frac{qB_{z0}}{2}(x^2 + y^2) = \text{Vector Potential Angular Momentum Term}$$

In S2E we plot for solenoidal focusing :

- Mechanical angular momentum $\propto xy' - yx'$
- Larmor rotation angle $\tilde{\psi}$
- Canonical angular momentum (constant) P_θ

Comments:

- Where valid, $P_\theta = \text{const}$ provides a powerful constraint to check dynamics
- If $P_\theta = \text{const}$ for all particles, then $\langle P_\theta \rangle = \text{const}$ for the beam as a whole and it is found in envelope models that canonical angular momentum can act effectively act phase-space area (emittance-like term) defocusing the beam
- Valid for acceleration: similar to a "normalized emittance": see S10

Example: solenoidal focusing channel

Employ the solenoid focusing channel example in S2E and plot:

- Mechanical angular momentum $\propto xy' - yx'$
- Vector potential contribution to canonical angular momentum $\propto B_{z0}(x^2 + y^2)$
- Canonical angular momentum (constant) P_θ

$$\frac{P_\theta}{m\gamma_b\beta_b c} = xy' - yx' + \frac{B_{z0}}{2[B\rho]}(x^2 + y^2) = \text{const} = \text{Canonical Angular Momentum}$$

$$xy' - yx' = r^2\theta' = \text{Mechanical Angular Momentum}$$

$$\frac{B_{z0}}{2[B\rho]}(x^2 + y^2) = \sqrt{\kappa}(x^2 + y^2) = \text{Vector Potential Component Canonical Angular Momentum}$$

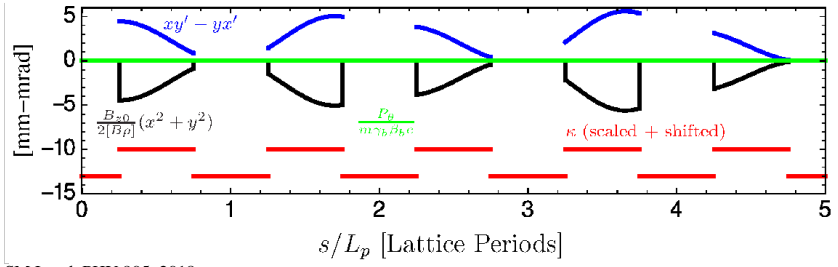

Comments on Orbits (see also info in S2E on 3D orbit):

- Mechanical angular momentum jumps discontinuously going into and out of the solenoid
  - Particle spins up (θ' jumps) and down going into and out of the solenoid
  - No mechanical angular momentum outside of solenoid due to the choice of intial condition in this example (initial x-plane motion)
- Canonical angular momentum P_θ is conserved in the 3D orbit evolution
  - Invariance provides a strong check on dynamics
  - P_θ in example has zero value due to the specific (x-plane) choice of initial condition of the particle. Other choices can give nonzero values and finite mechanical angular momentum in drifts.
- Solenoid provides focusing due to radial kicks associated with the "fringe" field entering the solenoid
  - Kick is abrupt for hard-edge solenoids
  - Details on radial kick/rotation structure can be found in Appendix C

Alternative expressions of canonical angular momentum

It is insightful to express the canonical angular momentum in (denoted tilde here) in the solenoid focusing canonical variables used earlier in this section and rotating Larmor frame variables:

- See Appendix B for Larmor frame transform
- Might expect simpler form of expressions given the relative simplicity of the formulation in canonical and Larmor frame variables

Canonical Variables:

$$\tilde{x} = x \qquad \tilde{y} = y$$

$$\tilde{x}' = x' - \frac{B_{z0}}{2[B\rho]} y \qquad \tilde{y}' = y' + \frac{B_{z0}}{2[B\rho]} x$$

$$\Longrightarrow \quad \boxed{\begin{aligned} \frac{P_\theta}{m\gamma_b\beta_b c} &\equiv xy' - yx' + \frac{B_{z0}}{2[B\rho]}(x^2 + y^2) \\ &= \tilde{x}\tilde{y}' - \tilde{x}\tilde{y}' \end{aligned}}$$

- Applies to acceleration also since just employing transform as a definition here

Larmor (Rotating) Frame Variables:

Larmor transform following formulation in Appendix B:

- Here tildes denote Larmor frame variables

$$\begin{bmatrix} x \\ x' \\ y \\ y' \end{bmatrix} = \begin{bmatrix} \cos\tilde{\psi} & 0 & -\sin\tilde{\psi} & 0 \\ k_L \sin\tilde{\psi} & \cos\tilde{\psi} & k_L\cos\tilde{\psi} & -\sin\tilde{\psi} \\ \sin\tilde{\psi} & 0 & \cos\tilde{\psi} & 0 \\ -k_L\cos\tilde{\psi} & \sin\tilde{\psi} & k_L\sin\tilde{\psi} & \cos\tilde{\psi} \end{bmatrix} \begin{bmatrix} \tilde{x} \\ \tilde{x}' \\ \tilde{y} \\ \tilde{y}' \end{bmatrix}$$

$$\tilde{\psi}(s) = -\int_{s_i}^{s} d\bar{s}\, k_L(\bar{s})$$

$$k_L(s) \equiv \frac{B_{z0}(s)}{2[B\rho]}$$

gives after some algebra:

$$\Longrightarrow \qquad x^2 + y^2 = \tilde{x}^2 + \tilde{y}^2$$

$$xy' - yx' = \tilde{x}\tilde{y}' - \tilde{y}\tilde{x}' - \frac{B_{z0}}{2[B\rho]}(\tilde{x}^2 + \tilde{y}^2)$$

Showing that:

$$\boxed{\begin{aligned} \frac{P_\theta}{m\gamma_b\beta_b c} &\equiv xy' - yx' + \frac{B_{z0}}{2[B\rho]}(x^2 + y^2) \\ &= \tilde{x}\tilde{y}' - \tilde{x}\tilde{y}' \end{aligned}}$$

- Same form as previous canonical variable case due to notation choices. However, steps/variables and implications different in this case !

Bush's Theorem expression of canonical angular momentum conservation

Take:

$$\boxed{\mathbf{B}^a = \nabla \times \mathbf{A}}$$

and apply Stokes Theorem to calculate the magnetic flux Ψ through a circle of radius r:

$$\boxed{\Psi = \int_r d^2x\, \mathbf{B}^a \cdot \hat{\mathbf{z}} = \int_r d^2x\, (\nabla \times \mathbf{A}) \cdot \hat{\mathbf{z}} = \oint_r \mathbf{A} \cdot d\vec{\ell}}$$

For a nonlinear, but axisymmetric solenoid, one can always take:

- Also applies to linear field component case

$$\mathbf{A} = \hat{\theta} A_\theta(r, z)$$

$$\Longrightarrow \quad \mathbf{B}^a = -\hat{\mathbf{r}} \frac{\partial A_\theta}{\partial z} + \hat{\mathbf{z}} \frac{1}{r} \frac{\partial}{\partial r} (r A_\theta)$$

Thus:

$$\boxed{\Psi = 2\pi r A_\theta}$$

// Aside: Nonlinear Application of Vector Potential

Given the magnetic field components

$$B_r^a(r,z) \qquad B_z^a(r,z)$$

the equations

$$B_r^a(r,z) = -\frac{\partial}{\partial z} A_\theta(r,z)$$
$$B_z^a(r,z) = \frac{1}{r}\frac{\partial}{\partial r}[rA_\theta(r,z)]$$

can be integrated for a single isolated magnet to obtain *equivalent* expressions for A_θ

$$A_\theta(r,z) = -\int_{-\infty}^{z} d\tilde{z}\; B_r^a(r,\tilde{z})$$
$$A_\theta(r,z) = \frac{1}{r}\int_0^r d\tilde{r}\tilde{r}\; B_z^a(\tilde{r},z)$$

- Resulting A_θ contains consistent nonlinear terms with magnetic field

//

Then the exact form of the canonical angular momentum for for solenoid focusing can be expressed as:

- Here γ factor is exact (not paraxial)

$$P_\theta = m\gamma r^2\dot{\theta} + qrA_\theta$$
$$= m\gamma r^2\dot{\theta} + \frac{q\Psi}{2\pi}$$

This form is often applied in solenoidal focusing and is known as "Bush's Theorem" with

$$\mathrm{P}_\theta = m\gamma r^2\dot{\theta} + \tfrac{q\Psi}{2\pi} = \mathrm{const}$$

- In a static applied magnetic field, $\gamma = \mathrm{const}$ further simplifying use of eqn
- Exact as expressed, but easily modified using familiar steps for paraxial form and/or linear field components
- Expresses how a particle "spins up" when entering a solenoidal magnetic field

Appendix A: Quadrupole Skew Coupling

Consider a quadrupole actively rotated through an angle ψ about the z-axis:

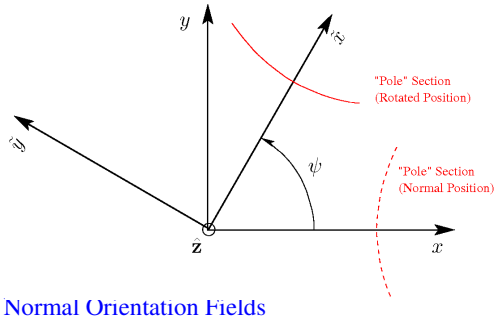

Transforms

$$\tilde{x} = \;\; x\cos\psi + y\sin\psi$$
$$\tilde{y} = -x\sin\psi + y\cos\psi$$

$$x = \;\; \tilde{x}\cos\psi - \tilde{y}\sin\psi$$
$$y = \;\; \tilde{x}\sin\psi + \tilde{y}\cos\psi$$

Normal Orientation Fields

Electric

$$E_x^a = -Gx$$
$$E_y^a = \;\; Gy$$

Magnetic

$$B_x^a = Gy$$
$$B_y^a = Gx$$

$G = G(s)$

= Field Gradient (Electric or Magnetic)

Note: units of G different in electric and magnetic cases

A1

Rotated Fields

Electric

$$E_x^a = E_{\tilde{x}}^a\cos\psi \;\; - \;\; E_{\tilde{y}}^a\sin\psi \qquad E_{\tilde{x}}^a = -G\tilde{x} = -G(\;\; x\cos\psi + y\sin\psi)$$
$$E_y^a = E_{\tilde{x}}^a\sin\psi \;\; + \;\; E_{\tilde{y}}^a\cos\psi \qquad E_{\tilde{y}}^a = \;\; G\tilde{y} = \;\; G(-x\sin\psi + y\cos\psi)$$

Combine equations, collect terms, and apply trigonometric identities to obtain:

$$E_x^a = -G\cos(2\psi)x - G\sin(2\psi)y$$
$$E_y^a = -G\sin(2\psi)x + G\cos(2\psi)y$$

$$2\sin\psi\cos\psi = \sin(2\psi)$$
$$\cos^2\psi - \sin^2\psi = \cos(2\psi)$$

Magnetic

$$B_x^a = B_{\tilde{x}}^a\cos\psi \;\; - \;\; B_{\tilde{y}}^a\sin\psi \qquad B_{\tilde{x}}^a = G\tilde{y} = G(-x\sin\psi + y\cos\psi)$$
$$B_y^a = B_{\tilde{x}}^a\sin\psi \;\; + \;\; B_{\tilde{y}}^a\cos\psi \qquad B_{\tilde{y}}^a = G\tilde{x} = G(\;\; x\cos\psi + y\sin\psi)$$

Combine equations, collect terms, and apply trigonometric identities to obtain:

$$B_x^a = -G\sin(2\psi)x + G\cos(2\psi)y$$
$$B_y^a = \;\; G\cos(2\psi)x + G\sin(2\psi)y$$

A2

For *both* electric and magnetic focusing quadrupoles, these field component projections can be inserted in the linear field Eqns of motion to obtain:

Skew Coupled Quadrupole Equations of Motion

$$x'' + \frac{(\gamma_b\beta_b)'}{(\gamma_b\beta_b)}x' + \kappa\cos(2\psi)x + \kappa\sin(2\psi)y = -\frac{q}{m\gamma_b^3\beta_b^2c^2}\frac{\partial\phi}{\partial x}$$

$$y'' + \frac{(\gamma_b\beta_b)'}{(\gamma_b\beta_b)}y' - \kappa\cos(2\psi)y + \kappa\sin(2\psi)x = -\frac{q}{m\gamma_b^3\beta_b^2c^2}\frac{\partial\phi}{\partial y}$$

$$\kappa = \begin{cases} \frac{G}{\beta_b c[B\rho]}, & \text{Electric Focusing} \\ \frac{G}{[B\rho]}, & \text{Magnetic Focusing} \end{cases}$$

System is skew coupled:

- x-equation depends on y, y' and y-equation on x, x' for $\psi \neq n\pi/2$ (n integer)

Skew-coupling considerably complicates dynamics

- Unless otherwise specified, we consider only quadrupoles with "normal" orientation with $\psi = n\pi/2$
- Skew coupling errors or intentional skew couplings can be important
  - Leads to transfer of oscillations energy between x and y-planes
  - Invariants much more complicated to construct/interpret

A3

The skew coupled equations of motion can be alternatively derived by actively rotating the quadrupole equation of motion in the form:

$$x'' + \frac{(\gamma_b\beta_b)'}{(\gamma_b\beta_b)}x' + \kappa(s)x = -\frac{q}{m\gamma_b^3\beta_b^2c^2}\frac{\partial\phi}{\partial x}$$

$$y'' + \frac{(\gamma_b\beta_b)'}{(\gamma_b\beta_b)}y' - \kappa(s)y = -\frac{q}{m\gamma_b^3\beta_b^2c^2}\frac{\partial\phi}{\partial y}$$

- Steps are then identical whether quadrupoles are electric *or* magnetic

A4

Appendix B: The Larmor Transform to Express Solenoidal Focused Particle Equations of Motion in Uncoupled Form

Solenoid equations of motion:

$$x'' + \frac{(\gamma_b\beta_b)'}{(\gamma_b\beta_b)}x' - \frac{B'_{z0}(s)}{2[B\rho]}y - \frac{B_{z0}(s)}{[B\rho]}y' = -\frac{q}{m\gamma_b^3\beta_b^2c^2}\frac{\partial\phi}{\partial x}$$

$$y'' + \frac{(\gamma_b\beta_b)'}{(\gamma_b\beta_b)}y' + \frac{B'_{z0}(s)}{2[B\rho]}x + \frac{B_{z0}(s)}{[B\rho]}x' = -\frac{q}{m\gamma_b^3\beta_b^2c^2}\frac{\partial\phi}{\partial y}$$

$$B_{z0}(s) = B_z^a(r=0, z=s) = \text{On-Axis Field}$$

$$[B\rho] = \frac{\gamma_b\beta_b mc}{q} = \text{Rigidity}$$

To simplify algebra, introduce the complex coordinate

$$\underline{z} \equiv x + iy \qquad i \equiv \sqrt{-1}$$

Note* context clarifies use of i (particle index, initial cond, complex i)

Then the two equations can be expressed as a single complex equation

$$\underline{z}'' + \frac{(\gamma_b\beta_b)'}{(\gamma_b\beta_b)}\underline{z}' + i\frac{B'_{z0}(s)}{2[B\rho]}\underline{z} + i\frac{B_{z0}(s)}{[B\rho]}\underline{z}' = -\frac{q}{m\gamma_b^3\beta_b^2c^2}\left(\frac{\partial\phi}{\partial x} + i\frac{\partial\phi}{\partial y}\right)$$

B1

If the potential is axisymmetric with $\phi = \phi(r)$:

$$\frac{\partial\phi}{\partial x} + i\frac{\partial\phi}{\partial y} = \frac{\partial\phi}{\partial r}\frac{\underline{z}}{r} \qquad r \equiv \sqrt{x^2+y^2}$$

then the complex form equation of motion reduces to:

$$\underline{z}'' + \frac{(\gamma_b\beta_b)'}{(\gamma_b\beta_b)}\underline{z}' + i\frac{B'_{z0}(s)}{2[B\rho]}\underline{z} + i\frac{B_{z0}(s)}{[B\rho]}\underline{z}' = -\frac{q}{m\gamma_b^3\beta_b^2c^2}\frac{\partial\phi}{\partial r}\frac{\underline{z}}{r}$$

Following Wiedemann, Vol II, pg 82, introduce a transformed complex variable that is a local (s-varying) rotation:

$$\tilde{\underline{z}} \equiv \underline{z}e^{-i\tilde{\psi}(s)} = \tilde{x} + i\tilde{y}$$

$\tilde{\psi}(s) =$ phase-function (real-valued)

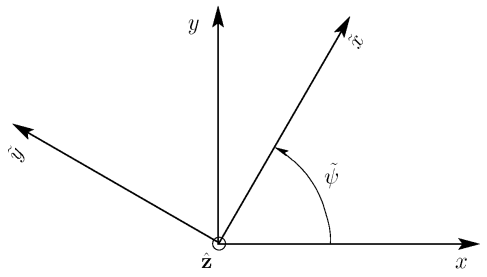

B2

Then: $\underline{z} = \tilde{\underline{z}} e^{i\tilde{\psi}}$

$$\underline{z}' = \left(\tilde{\underline{z}}' + i\tilde{\psi}'\tilde{\underline{z}}\right) e^{i\tilde{\psi}}$$

$$\underline{z}'' = \left(\tilde{\underline{z}}'' + 2i\tilde{\psi}'\tilde{\underline{z}}' + i\tilde{\psi}''\tilde{\underline{z}} - \tilde{\psi}'^2\tilde{\underline{z}}\right) e^{i\tilde{\psi}}$$

and the complex form equations of motion become:

$$\tilde{\underline{z}}'' + \left[i\left(2\tilde{\psi}' + \frac{B_{z0}}{[B\rho]}\right) + \frac{(\gamma_b\beta_b)'}{(\gamma_b\beta_b)}\right]\tilde{\underline{z}}' + \left[-\tilde{\psi}'^2 - \frac{B_{z0}}{[B\rho]}\tilde{\psi}' + i\left(\tilde{\psi}'' + \frac{B'_{z0}}{2[B\rho]} + \frac{(\gamma_b\beta_b)'}{(\gamma_b\beta_b)}\tilde{\psi}'\right)\right]\tilde{\underline{z}} = -\frac{q}{m\gamma_b^3\beta_b^2c^2}\frac{\partial\phi}{\partial r}\frac{\tilde{\underline{z}}}{r}$$

Free to choose the form of $\tilde{\psi}$ Can choose to eliminate imaginary terms in $i($ .... $)$ in equation by taking:

$$\tilde{\psi}' \equiv -\frac{B_{z0}}{2[B\rho]} \quad \Longrightarrow \quad \tilde{\psi}'' = -\frac{B'_{z0}}{2[B\rho]} + \frac{B_{z0}}{2[B\rho]}\frac{(\gamma_b\beta_b)'}{(\gamma_b\beta_b)}$$

B3

Using these results, the complex form equations of motion reduce to: B4

$$\tilde{\underline{z}}'' + \frac{(\gamma_b\beta_b)'}{(\gamma_b\beta_b)}\tilde{\underline{z}}' + \left(\frac{B_{z0}}{2[B\rho]}\right)^2\tilde{\underline{z}} = -\frac{q}{m\gamma_b^3\beta_b^2c^2}\frac{\partial\phi}{\partial r}\frac{\tilde{\underline{z}}}{r}$$

Or using $\tilde{\underline{z}} = \tilde{x} + i\tilde{y}$, the equations can be expressed in decoupled $\tilde{x}$, $\tilde{y}$ variables in the Larmor Frame as:

$$\tilde{x}'' + \frac{(\gamma_b\beta_b)'}{(\gamma_b\beta_b)}\tilde{x}' + \kappa(s)\tilde{x} = -\frac{q}{m\gamma_b^3\beta_b^2c^2}\frac{\partial\phi}{\partial r}\frac{\tilde{x}}{r}$$

$$\tilde{y}'' + \frac{(\gamma_b\beta_b)'}{(\gamma_b\beta_b)}\tilde{y}' + \kappa(s)\tilde{y} = -\frac{q}{m\gamma_b^3\beta_b^2c^2}\frac{\partial\phi}{\partial r}\frac{\tilde{y}}{r}$$

$$\kappa(s) \equiv k_L^2(s) \qquad k_L(s) \equiv \frac{B_{z0}(s)}{2[B\rho]} = \frac{\omega_c(s)}{2\gamma_b\beta_bc} \qquad [B\rho] = \frac{\gamma_b\beta_bmc}{q}$$

$$= \text{Larmor Wave-Number}$$

Equations of motion are uncoupled but must be interpreted in the rotating Larmor frame

- Same form as quadrupoles but with focusing function same sign in each plane

The rotational transformation to the Larmor Frame can be effected by integrating the equation for $\tilde{\psi}' = -\frac{B_{z0}}{2[B\rho]}$

$$\tilde{\psi}(s) = -\int_{s_i}^{s} d\tilde{s}\,\frac{B_{z0}(\tilde{s})}{2[B\rho]} = -\int_{s_i}^{s} d\tilde{s}\,k_L(\tilde{s})$$

Here, s_i is some value of s where the initial conditions are taken.

- Take $s = s_i$ where axial field is zero for simplest interpretation (see: pg B6)

Because

$$\tilde{\psi}' = -\frac{B_{z0}}{2[B\rho]} = \frac{\omega_c}{2\gamma_b\beta_bc}$$

the local $\tilde{x} - \tilde{y}$ Larmor frame is rotating at ½ of the local s-varying cyclotron frequency

- If $B_{z0} = \text{const}$, then the Larmor frame is uniformly rotating as is well known from elementary textbooks (see problem sets)

B5

The complex form phase-space transformation and inverse transformations are:

$$\underline{z} = \tilde{\underline{z}}e^{i\tilde{\psi}} \qquad \tilde{\underline{z}} = \underline{z}e^{-i\tilde{\psi}}$$

$$\underline{z}' = \left(\tilde{\underline{z}}' + i\tilde{\psi}'\tilde{\underline{z}}\right)e^{i\tilde{\psi}} \qquad \tilde{\underline{z}}' = \left(\underline{z}' - i\tilde{\psi}'\underline{z}\right)e^{-i\tilde{\psi}}$$

$$\underline{z} = x + iy \qquad \tilde{\underline{z}} = \tilde{x} + i\tilde{y} \qquad \tilde{\psi}' = -k_L$$

$$\underline{z}' = x' + iy' \qquad \tilde{\underline{z}}' = \tilde{x}' + i\tilde{y}'$$

Apply to:

- Project initial conditions from lab-frame when integrating equations
- Project integrated solution back to lab-frame to interpret solution

If the initial condition $s = s_i$ is taken outside of the magnetic field where $B_{z0}(s_i) = 0$, then:

$$\tilde{x}(s = s_i) = x(s = s_i) \qquad \tilde{x}'(s = s_i) = x'(s = s_i)$$

$$\tilde{y}(s = s_i) = y(s = s_i) \qquad \tilde{y}'(s = s_i) = y'(s = s_i)$$

$$\tilde{\underline{z}}(s = s_i) = \underline{z}(s = s_i) \qquad \tilde{\underline{z}}'(s = s_i) = \underline{z}'(s = s_i)$$

B6

The transform and inverse transform between the laboratory and rotating frames can then be applied to project initial conditions into the rotating frame for integration and then the rotating frame solution back into the laboratory frame.

Using the real and imaginary parts of the complex-valued transformations:

$$\begin{bmatrix} x \\ x' \\ y \\ y' \end{bmatrix} = \tilde{\mathbf{M}}_r(s|s_i) \cdot \begin{bmatrix} \tilde{x} \\ \tilde{x}' \\ \tilde{y} \\ \tilde{y}' \end{bmatrix} \qquad \begin{bmatrix} \tilde{x} \\ \tilde{x}' \\ \tilde{y} \\ \tilde{y}' \end{bmatrix} = \tilde{\mathbf{M}}_r^{-1}(s|s_i) \cdot \begin{bmatrix} x \\ x' \\ y \\ y' \end{bmatrix}$$

$$\tilde{\mathbf{M}}_r(s|s_i) = \begin{bmatrix} \cos\tilde{\psi} & 0 & -\sin\tilde{\psi} & 0 \\ k_L \sin\tilde{\psi} & \cos\tilde{\psi} & k_L\cos\tilde{\psi} & -\sin\tilde{\psi} \\ \sin\tilde{\psi} & 0 & \cos\tilde{\psi} & 0 \\ -k_L\cos\tilde{\psi} & \sin\tilde{\psi} & k_L\sin\tilde{\psi} & \cos\tilde{\psi} \end{bmatrix}$$

$$\tilde{\mathbf{M}}_r^{-1}(s|s_i) = \begin{bmatrix} \cos\tilde{\psi} & 0 & \sin\tilde{\psi} & 0 \\ k_L \sin\tilde{\psi} & \cos\tilde{\psi} & -k_L\cos\tilde{\psi} & \sin\tilde{\psi} \\ -\sin\tilde{\psi} & 0 & \cos\tilde{\psi} & 0 \\ k_L\cos\tilde{\psi} & -\sin\tilde{\psi} & k_L\sin\tilde{\psi} & \cos\tilde{\psi} \end{bmatrix}$$

Here we used:

$$\tilde{\psi}' = -k_L$$

and it can be verified that:

$$\tilde{\mathbf{M}}_r^{-1} = \text{Inverse}[\tilde{\mathbf{M}}_r]$$

B7

Appendix C: Transfer Matrices for Hard-Edge Solenoidal Focusing

Using results and notation from Appendix B, derive transfer matrix for single particle orbit with:

- No space-charge
- No momentum spread

- Details of decompositions can be found in: Conte and Mackay, "An Introduction to the Physics of Particle Accelerators" (2nd edition; 2008)

First, the solution to the Larmor-frame equations of motion:

$$\tilde{x}'' + \frac{(\gamma_b\beta_b)'}{(\gamma_b\beta_b)}\tilde{x}' + \kappa(s)\tilde{x} = 0$$

$$\tilde{y}'' + \frac{(\gamma_b\beta_b)'}{(\gamma_b\beta_b)}\tilde{y}' + \kappa(s)\tilde{y} = 0$$

$$\kappa = k_L^2 = \left(\frac{B_{z0}}{2[B\rho]}\right)^2$$

Can be expressed as:

$$\begin{bmatrix} \tilde{x} \\ \tilde{x}' \\ \tilde{y} \\ \tilde{y}' \end{bmatrix}_z = \tilde{\mathbf{M}}_L(z|z_i) \cdot \begin{bmatrix} \tilde{x} \\ \tilde{x}' \\ \tilde{y} \\ \tilde{y}' \end{bmatrix}_{z=z_i}$$

- In this appendix we use z rather than s for the axial coordinate since there are not usually bends in a solenoid

C1

Transforming the solution back to the laboratory frame:

$$\begin{bmatrix} x \\ x' \\ y \\ y' \end{bmatrix}_z = \tilde{\mathbf{M}}_r(z|z_i) \cdot \tilde{\mathbf{M}}_L(z|z_i) \cdot \tilde{\mathbf{M}}_r^{-1}(z_i|z_i) \cdot \begin{bmatrix} x \\ x' \\ y \\ y' \end{bmatrix}_{z=z_i}$$

From project of initial conditions to Larmor Frame

$$= I \text{ Identity Matrix}$$

- Here we assume the initial condition is outside the magnetic field so that there is no adjustment to the Larmor frame angles, i.e., $\tilde{\mathbf{M}}_r^{-1}(z_i|z_i) = \mathbf{I}$

$$\begin{bmatrix} x \\ x' \\ y \\ y' \end{bmatrix}_z \equiv \mathbf{M}(z|z_i) \cdot \begin{bmatrix} x \\ x' \\ y \\ y' \end{bmatrix}_{z=z_i} = \tilde{\mathbf{M}}_r(z|z_i) \cdot \tilde{\mathbf{M}}_L(z|z_i) \cdot \begin{bmatrix} x \\ x' \\ y \\ y' \end{bmatrix}_{z=z_i}$$

$$\mathbf{M}(z|z_i) = \tilde{\mathbf{M}}_r(z|z_i) \cdot \tilde{\mathbf{M}}_L(z|z_i)$$

- Care must be taken when applying to discontinuous (hard-edge) field models of solenoids to correctly calculate transfer matrices
  - Fringe field influences beam "spin-up" and "spin-down" entering and exiting the magnet

C2

Apply formulation to a hard-edge solenoid with no acceleration [$(\gamma_b\beta_b)' = 0$]:

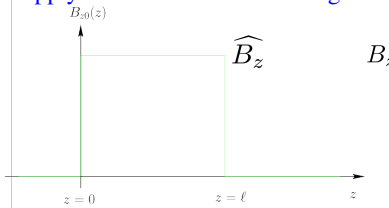

$$B_{z0}(z) = \widehat{B_z}\,[\Theta(z) - \Theta(z-\ell)]$$

$\widehat{B_z}$ = const = Hard-Edge Field

ℓ = const = Hard-Edge Magnet Length

Note coordinate choice: z=0 is start of magnet

Calculate the Larmor-frame transfer matrix in $0 \le z \le \ell$:

$$\tilde{x}'' + k_L^2\tilde{x} = 0$$

$$\tilde{y}'' + k_L^2\tilde{y} = 0$$

$$k_L = \frac{qB_{z0}}{2\gamma_b\beta_b mc} = \frac{B_{z0}}{2[B\rho]} = \frac{\widehat{B_z}}{2[B\rho]} = \text{const}$$

$0^- \le z \le \ell^+$

$$\tilde{\mathbf{M}}_L(z|0^-) = \begin{bmatrix} C & S/k_L & 0 & 0 \\ -k_L S & C & 0 & 0 \\ 0 & 0 & C & S/k_L \\ 0 & 0 & -k_L S & C \end{bmatrix}$$

$$C \equiv \cos(k_L z) \qquad S \equiv \sin(k_L z)$$

Subtle Point:

Larmor frame transfer matrix is valid both sides of discontinuity in focusing entering and exiting solenoid.

C3

The Larmor-frame transfer matrix can be decomposed as:

- Useful for later constructs

$$\tilde{\mathbf{M}}_L(z|0^-) = \begin{bmatrix} C & S/k_L & 0 & 0 \\ -k_L S & C & 0 & 0 \\ 0 & 0 & C & S/k_L \\ 0 & 0 & -k_L S & C \end{bmatrix} = \begin{bmatrix} \mathbf{F}(z) & \mathbf{0} \\ \mathbf{0} & \mathbf{F}(z) \end{bmatrix}$$

with

$$\tilde{\mathbf{F}}(z) \equiv \begin{bmatrix} C(z) & S(z)/k_L \\ -k_L S(z) & C(z) \end{bmatrix} \qquad \mathbf{0} \equiv \begin{bmatrix} 0 & 0 \\ 0 & 0 \end{bmatrix}$$

Using results from Appendix E, ***F*** can be further decomposed as:

$$\begin{aligned} \tilde{\mathbf{F}}(z) &= \begin{bmatrix} C(z) & S(z)/k_L \\ -k_L S(z) & C(z) \end{bmatrix} \\ &= \begin{bmatrix} 1 & \frac{1}{k_L}\tan\left(\frac{k_L z}{2}\right) \\ 0 & 1 \end{bmatrix} \cdot \begin{bmatrix} 1 & 0 \\ -k_L \sin(k_L z) & 1 \end{bmatrix} \cdot \begin{bmatrix} 1 & \frac{1}{k_L}\tan\left(\frac{k_L z}{2}\right) \\ 0 & 1 \end{bmatrix} \\ &= \mathbf{M}_{\text{drift}}(z) \cdot \mathbf{M}_{\text{thin-lens}}(z) \cdot \mathbf{M}_{\text{drift}}(z) \end{aligned}$$

C4

Applying these results and the formulation of Appendix B, we obtain the rotation matrix within the magnet $0 < z < \ell$:

- Here we apply $\tilde{\mathbf{M}}_r$ formula with $\tilde{\psi} = -k_L z$ for the hard-edge solenoid

$$\tilde{\mathbf{M}}_r(z|0^-) = \begin{bmatrix} C & 0 & S & 0 \\ -k_L S & C & k_L C & S \\ -S & 0 & C & 0 \\ -k_L C & -S & -k_L S & C \end{bmatrix}$$

Comment: Careful with minus signs! Here, C and S here have positive arguments as defined.

With special magnet end-forms:

- Here we exploit continuity of $\tilde{\mathbf{M}}_r$ in Larmor frame

Entering solenoid

$$\tilde{\mathbf{M}}_r(0^+|0^-) = \begin{bmatrix} 1 & 0 & 0 & 0 \\ 0 & 1 & k_L & 0 \\ 0 & 0 & 1 & 0 \\ -k_L & 0 & 0 & 1 \end{bmatrix}$$

- Direct plug-in from formula above for $\tilde{\mathbf{M}}_r$ at $z = 0^+$

Exiting solenoid

$$\tilde{\mathbf{M}}_r(\ell^+|\ell^-) = \begin{bmatrix} 1 & 0 & 0 & 0 \\ 0 & 1 & -k_L & 0 \\ 0 & 0 & 1 & 0 \\ k_L & 0 & 0 & 1 \end{bmatrix}$$

- Slope of fringe field is reversed so replace in entrance formula: $k_L \to -k_L$

C5

The rotation matrix through the full solenoid is (plug in to previous formula for $\tilde{\mathbf{M}}_r(z|0^-)$):

$$\tilde{\mathbf{M}}_r(\ell + |0^-) = \begin{bmatrix} \cos\Phi & 0 & \sin\Phi & 0 \\ 0 & \cos\Phi & 0 & \sin\Phi \\ -\sin\Phi & 0 & \cos\Phi & 0 \\ 0 & -\sin\Phi & 0 & \cos\Phi \end{bmatrix} = \begin{bmatrix} \mathbf{I}\cos\Phi & \mathbf{I}\sin\Phi \\ -\mathbf{I}\sin\Phi & \mathbf{I}\cos\Phi \end{bmatrix}$$

$$\Phi \equiv k_L \ell \qquad \mathbf{I} \equiv \begin{bmatrix} 1 & 0 \\ 0 & 1 \end{bmatrix}$$

and the rotation matrix within the solenoid is (plug into formula for $\tilde{\mathbf{M}}_r(z|0^-)$ and apply algebra to resolve sub-forms):

$$\begin{aligned} \tilde{\mathbf{M}}_r(z|0^-) &= \begin{bmatrix} C(z) & 0 & S(z) & 0 \\ 0 & C(z) & 0 & S(z) \\ -S(z) & 0 & C(z) & 0 \\ 0 & -S(z) & 0 & C(z) \end{bmatrix} \cdot \begin{bmatrix} 1 & 0 & 0 & 0 \\ 0 & 1 & k_L & 0 \\ 0 & 0 & 1 & 0 \\ -k_L & 0 & 0 & 1 \end{bmatrix} \\ &= \begin{bmatrix} C(z)\mathbf{I} & S(z)\mathbf{I} \\ -S(z)\mathbf{I} & C(z)\mathbf{I} \end{bmatrix} \cdot \begin{bmatrix} \mathbf{I} & \mathbf{K} \\ -\mathbf{K} & \mathbf{I} \end{bmatrix} \qquad \mathbf{K} \equiv \begin{bmatrix} 0 & 0 \\ k_L & 0 \end{bmatrix} \\ &= \tilde{\mathbf{M}}_r(z|0^+) \cdot \tilde{\mathbf{M}}_r(0^+|0^-) \qquad 0 < z < \ell \end{aligned}$$

Note that the rotation matrix kick entering the solenoid is expressible as

$$\tilde{\mathbf{M}}_r(0^+|0^-) = \begin{bmatrix} \mathbf{I} & \mathbf{K} \\ -\mathbf{K} & \mathbf{I} \end{bmatrix}$$

C6

The lab-frame advance matrices are then (after expanding matrix products):

Inside Solenoid $0^+ \le z \le \ell^-$

$$\begin{aligned} \mathbf{M}(z|0^-) &= \tilde{\mathbf{M}}_r(z|0^-)\tilde{\mathbf{M}}_L(z|0^-) \\ &= \begin{bmatrix} \cos^2\phi & \frac{1}{2k_L}\sin(2\phi) & \frac{1}{2}\sin(2\phi) & \frac{1}{k_L}\sin^2\phi \\ -k_L\sin(2\phi) & \cos(2\phi) & k_L\cos(2\phi) & \sin(2\phi) \\ -\frac{1}{2}\sin(2\phi) & -\frac{1}{k_L}\sin^2\phi & \cos^2\phi & \frac{1}{2k_L}\sin(2\phi) \\ -k_L\cos(2\phi) & -\sin(2\phi) & -k_L\sin(2\phi) & \cos(2\phi) \end{bmatrix} \\ &\quad \phi \equiv k_L z \\ &= \begin{bmatrix} C(z)\mathbf{I} & S(z)\mathbf{I} \\ -S(z)\mathbf{I} & C(z)\mathbf{I} \end{bmatrix} \cdot \begin{bmatrix} \mathbf{I} & \mathbf{K} \\ -\mathbf{K} & \mathbf{I} \end{bmatrix} \cdot \begin{bmatrix} \mathbf{F}(z) & \mathbf{0} \\ \mathbf{0} & \mathbf{F}(z) \end{bmatrix} \\ &= \begin{bmatrix} C(z)\mathbf{I} - S(z)\mathbf{K} & C(z)\mathbf{K} + S(z)\mathbf{I} \\ -C(z)\mathbf{K} - S(z)\mathbf{I} & C(z)\mathbf{I} - S(z)\mathbf{K} \end{bmatrix} \cdot \begin{bmatrix} \mathbf{F}(z) & \mathbf{0} \\ \mathbf{0} & \mathbf{F}(z) \end{bmatrix} \\ &= \begin{bmatrix} C(z)\mathbf{F}(z) - S(z)\mathbf{K}\cdot\mathbf{F}(z) & C(z)\mathbf{K}\cdot\mathbf{F}(z) + S(z)\mathbf{F}(z) \\ -C(z)\mathbf{K}\cdot\mathbf{F}(z) - S(z)\mathbf{F}(z) & C(z)\mathbf{F}(z) - S(z)\mathbf{K}\cdot\mathbf{F}(z) \end{bmatrix} \end{aligned}$$

- 2nd forms useful to see structure of transfer matrix

C7

Through entire Solenoid $z = \ell^+$

$$\mathbf{M}(\ell^+|0^-) = \tilde{\mathbf{M}}_r(\ell^+|0^-)\tilde{\mathbf{M}}_L(\ell^+|0^-)$$

$$= \begin{bmatrix} \cos^2\Phi & \frac{1}{2k_L}\sin(2\Phi) & \frac{1}{2}\sin(2\Phi) & \frac{1}{k_L}\sin^2\Phi \\ -\frac{k_L}{2}\sin(2\Phi) & \cos^2\Phi & -k_L\sin^2\Phi & \frac{1}{2}\sin(2\Phi) \\ -\frac{1}{2}\sin(2\Phi) & -\frac{1}{k_L}\sin^2\Phi & \cos^2\Phi & \frac{1}{2k_L}\sin(2\Phi) \\ k_L\sin^2\Phi & -\frac{1}{2}\sin(2\Phi) & -\frac{k_L}{2}\sin(2\Phi) & \cos^2\Phi \end{bmatrix}$$

$$\Phi \equiv k_L\ell$$

$$= \begin{bmatrix} \cos\Phi\mathbf{I} & \sin\Phi\mathbf{I} \\ -\sin\Phi\mathbf{I} & \cos\Phi\mathbf{I} \end{bmatrix} \cdot \begin{bmatrix} \mathbf{F}(\ell) & \mathbf{0} \\ \mathbf{0} & \mathbf{F}(\ell) \end{bmatrix}$$

$$= \begin{bmatrix} \cos\Phi\mathbf{F}(\ell) & \sin\Phi\mathbf{F}(\ell) \\ -\sin\Phi\mathbf{F}(\ell) & \cos\Phi\mathbf{F}(\ell) \end{bmatrix}$$

- 2nd forms useful to see structure of transfer matrix

Note that due to discontinuous fringe field:

$$\mathbf{M}(0^+|0^-) = \begin{bmatrix} 1 & 0 & 0 & 0 \\ 0 & 1 & k_L & 0 \\ 0 & 0 & 1 & 0 \\ -k_L & 0 & 0 & 1 \end{bmatrix} = \begin{bmatrix} \mathbf{I} & \mathbf{K} \\ -\mathbf{K} & \mathbf{I} \end{bmatrix} \neq I$$

Fringe going in kicks angles of beam

C8

$$\mathbf{M}(\ell^-|0^-) \neq \mathbf{M}(\ell^+|0^-)$$

Due to fringe exiting kicking angles of beam

In more realistic model with a continuously varying fringe to zero, all transfer matrix components will vary continuously across boundaries

- Still important to get this right in idealized designs often taken as a first step!

Focusing kicks on particles entering/exiting the solenoid can be calculated as:

Entering:

$$\begin{aligned} x(0^+) &= x(0^-) & x'(0^+) &= x'(0^-) + k_L y(0^-) \\ y(0^+) &= y(0^-) & y'(0^+) &= y'(0^-) - k_L x(0^-) \end{aligned}$$

Exiting:

$$\begin{aligned} x(\ell^+) &= x(\ell^-) & x'(\ell^+) &= x'(\ell^-) - k_L y(\ell^-) \\ y(\ell^+) &= y(\ell^-) & y'(\ell^+) &= y'(\ell^-) + k_L x(\ell^-) \end{aligned}$$

- Beam spins up/down on entering/exiting the (abrupt) magnetic fringe field
- Sense of rotation changes with entry/exit of hard-edge field.

C9

The transfer matrix for a hard-edge solenoid can be resolved into thin-lens kicks entering and exiting the optic and an rotation in the central region of the optic as:

$$\mathbf{M}(\ell^+|0^-) = \tilde{\mathbf{M}}_r(\ell^+|0^-)\tilde{\mathbf{M}}_L(\ell^+|0^-)$$

$$= \begin{bmatrix} \cos^2\Phi & \frac{1}{2k_L}\sin(2\Phi) & \frac{1}{2}\sin(2\Phi) & \frac{1}{k_L}\sin^2\Phi \\ -\frac{k_L}{2}\sin(2\Phi) & \cos^2\Phi & -k_L\sin^2\Phi & \frac{1}{2}\sin(2\Phi) \\ -\frac{1}{2}\sin(2\Phi) & -\frac{1}{k_L}\sin^2\Phi & \cos^2\Phi & \frac{1}{2k_L}\sin(2\Phi) \\ k_L\sin^2\Phi & -\frac{1}{2}\sin(2\Phi) & -\frac{k_L}{2}\sin(2\Phi) & \cos^2\Phi \end{bmatrix}$$

$$= \begin{bmatrix} 1 & 0 & 0 & 0 \\ 0 & 1 & -k_L & 0 \\ 0 & 0 & 1 & 0 \\ k_L & 0 & 0 & 1 \end{bmatrix} \begin{bmatrix} 1 & \frac{1}{2k_L}\sin(2\Phi) & 0 & \frac{1}{k_L}\sin^2\Phi \\ 0 & \cos(2\Phi) & 1 & \sin(2\Phi) \\ 0 & \frac{1}{k_L}\sin^2\Phi & 1 & \frac{1}{2k_L}\sin(2\Phi) \\ 1 & -\sin(2\Phi) & 0 & \cos(2\Phi) \end{bmatrix} \begin{bmatrix} 1 & 0 & 0 & 0 \\ 0 & 1 & k_L & 0 \\ 0 & 0 & 1 & 0 \\ -k_L & 0 & 0 & 1 \end{bmatrix}$$

$$= \mathbf{M}(\ell^+|\ell^-) \cdot \mathbf{M}(\ell^-|0^+) \cdot \mathbf{M}(0^+|0^-)$$

where $\Phi \equiv k_L\ell$

- Focusing effect effectively from thin lens kicks at entrance/exit of solenoid as particle traverses the (abrupt here) fringe field

C10

The transfer matrix for the hard-edge solenoid is exact within the context of linear optics. However, real solenoid magnets have an axial fringe field. An obvious need is how to best set the hard-edge parameters B_z, ℓ from the real fringe field.

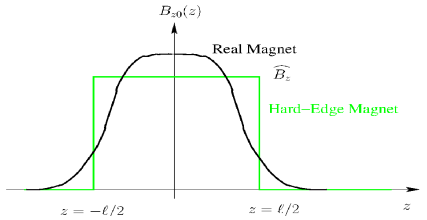

Hard-Edge and Real Magnets axially centered to compare

Simple physical motivated prescription by requiring:

1) Equivalent Linear Focus Impulse $\propto \int dz\, k_L^2 \propto \int dz B_{z0}^2$

$$\Longrightarrow \boxed{\int_{-\infty}^{\infty} dz\, B_{z0}^2(z) = \ell\widehat{B_z}^2}$$

2) Equivalent Net Larmor Rotation Angle $\propto \int dz\, k_L \propto \int dz\, B_{z0}$

$$\Longrightarrow \boxed{\int_{-\infty}^{\infty} dz\, B_{z0}(z) = \ell\widehat{B_z}}$$

C11

Solve 1) and 2) for harde edge parameters $\widehat{B_z},\ \ell$

$$\widehat{B_z} = \frac{\int_{-\infty}^{\infty} dz\ B_{z0}^2(z)}{\int_{-\infty}^{\infty} dz\ B_{z0}(z)}$$

$$\ell = \frac{\left[\int_{-\infty}^{\infty} dz\ B_{z0}(z)\right]^2}{\int_{-\infty}^{\infty} dz\ B_{z0}^2(z)}$$

C12

Appendix D: Axisymmetric Applied Magnetic or Electric Field Expansion

Static, rationally symmetric static applied fields $\mathbf{E}^a,\ \mathbf{B}^a$ satisfy the vacuum Maxwell equations in the beam aperture:

$$\nabla\cdot\mathbf{E}^a = 0 \qquad \nabla\times\mathbf{E}^a = 0 \qquad \nabla\cdot\mathbf{B}^a = 0 \qquad \nabla\times\mathbf{B}^a = 0$$

This implies we can take for some electric potential ϕ^e and magnetic potential ϕ^m:

$$\mathbf{E}^a = -\nabla\phi^e \qquad \mathbf{B}^a = -\nabla\phi^m$$

which in the vacuum aperture satisfies the Laplace equations:

$$\nabla^2\phi^e = 0 \qquad \nabla^2\phi^m = 0$$

We will analyze the magnetic case and the electric case is analogous. In axisymmetric $(\partial/\partial\theta = 0)$ geometry we express Laplace's equation as:

$$\nabla^2\phi^m(r,z) = \frac{1}{r}\frac{\partial}{\partial r}\left(r\frac{\partial\phi^m}{\partial r}\right) + \frac{\partial^2\phi^m}{\partial z^2} = 0$$

$\phi^m(r,z)$ can be expanded as (odd terms in r would imply nonzero $B_r = -\frac{\partial\phi_m}{\partial r}$ at $r = 0$):

$$\phi^m(r,z) = \sum_{\nu=0}^{\infty} f_{2\nu}(z) r^{2\nu} = f_0 + f_2 r^2 + f_4 r^4 + \ldots$$

where $f_0 = \phi^m(r=0,z)$ is the on-axis potential

D1

Plugging ϕ^m into Laplace's equation yields the recursion relation for $f_{2\nu}$

$$(2\nu+2)^2 f_{2\nu+2} + f''_{2\nu} = 0$$

Iteration then shows that

$$\phi^m(r,z) = \sum_{\nu=0}^{\infty} \frac{(-1)^\nu}{(\nu!)^2}\frac{\partial^{2\nu} f(0,z)}{\partial z^{2\nu}}\left(\frac{r}{2}\right)^{2\nu}$$

Using $B_z^a(r=0,z) \equiv B_{z0}(z) = -\dfrac{\partial\phi_m(0,z)}{\partial z}$ and diffrentiating yields:

$$B_r^a(r,z) = -\frac{\partial\phi_m}{\partial r} = \sum_{\nu=1}^{\infty} \frac{(-1)^\nu}{(\nu!)(\nu-1)!}\frac{\partial^{2\nu-1} B_{z0}(z)}{\partial z^{2\nu-1}}\left(\frac{r}{2}\right)^{2\nu-1}$$

$$B_z^a(r,z) = -\frac{\partial\phi_m}{\partial z} = \sum_{\nu=0}^{\infty} \frac{(-1)^\nu}{(\nu!)^2}\frac{\partial^{2\nu} B_{z0}(z)}{\partial z^{2\nu}}\left(\frac{r}{2}\right)^{2\nu}$$

- Electric case immediately analogous and can arise in electrostatic Einzel lens focusing systems often employed near injectors
- Electric case can also be applied to RF and induction gap structures in the quasistatic (long RF wavelength relative to gap) limit.

D2

Appendix E: Thin Lens Equivalence for Thick Lenses

In the thin lens model for an orbit described by Hill's equation:

$$x''(s) + \kappa_x(s)x(s) = 0$$

the applied focusing function $\kappa_x(s)$ is replaced by a "thin-lens" kick described by:

$$\kappa_x(s) = \frac{1}{f}\delta(s-s_0) \qquad \begin{array}{l} s_0 = \text{Optic Location} = \text{const} \\ f = \text{focal length} = \text{const} \end{array}$$

The transfer matrix to describe the action of the thin lens is found by integrating the Hills's equation to be:

$$\begin{bmatrix} x \\ x' \end{bmatrix}_{s=s_0^+} = \begin{bmatrix} 1 & 0 \\ -1/f & 1 \end{bmatrix} \cdot \begin{bmatrix} x \\ x' \end{bmatrix}_{s=s_0^-} \equiv \mathbf{M}_{\text{kick}} \begin{bmatrix} x \\ x' \end{bmatrix}_{s=s_0^-}$$

Graphical Interpretation:

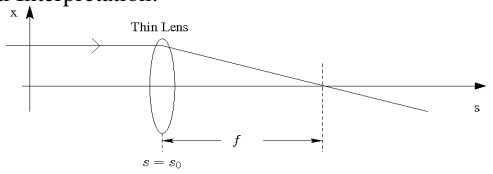

E1

For a free drift, Hill's equation is:

$$x''(s) = 0$$

with a corresponding transfer matrix solution:

$$\begin{bmatrix} x \\ x' \end{bmatrix}_s = \begin{bmatrix} 1 & (s-s_i) \\ 0 & 1 \end{bmatrix} \cdot \begin{bmatrix} x \\ x' \end{bmatrix}_{s_i} \equiv \mathbf{M}_{\text{drift}} \begin{bmatrix} x \\ x' \end{bmatrix}_{s_i}$$

We will show that the thin lens and two drifts can *exactly* replace

Case 1) Piecewise constant focusing lens: $\kappa_x(s) = \kappa = \text{const} > 0$

Case 2) Piecewise constant defocusing lens: $\kappa_x(s) = -\kappa = \text{const} < 0$

Case 3) Arbitrary linear lens represented by: $\kappa_x(s)$

This can be helpful since the thin lens + drift model is simple both to carry out algebra and conceptually understand.

E2

Case 1) The piecewise constant focusing transfer matrix $\mathbf{M}_x$ for $\kappa_x = \kappa > 0$ can be resolved as:

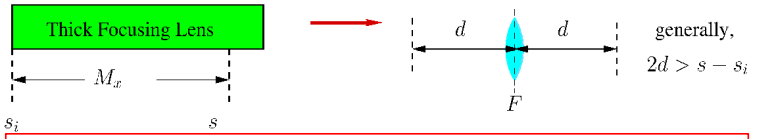

$$\mathbf{M_x}(s|s_i) = \begin{bmatrix} C(s) & S(s)/\sqrt{\kappa} \\ -\sqrt{\kappa}S(s) & C(s) \end{bmatrix} = \begin{bmatrix} 1 & d(s) \\ 0 & 1 \end{bmatrix} \cdot \begin{bmatrix} 1 & 0 \\ -1/f(s) & 1 \end{bmatrix} \cdot \begin{bmatrix} 1 & d(s) \\ 0 & 1 \end{bmatrix} \equiv \mathbf{M}_{\text{drift}} \cdot \mathbf{M}_{\text{kick}} \cdot \mathbf{M}_{\text{drift}}$$

where $C(s) = \cos[\sqrt{\kappa}(s-s_i)]$ $\quad d(s) = \tan[\sqrt{\kappa}(s-s_i)/2]/\sqrt{\kappa}$

$S(s) = \sin[\sqrt{\kappa}(s-s_i)]$ $\quad 1/f(s) = \sqrt{\kappa}S(s)$

This resolves the thick focusing lens into a thin-lens kick $\mathbf{M}_{\text{kick}}$ between two equal length drifts $\mathbf{M}_{\text{drift}}$ upstream and downstream of the kick

- Result specifies *exact* thin-lens equivalent focusing element
- Can also be applied to continuous focusing (in interval) and solenoid focusing (in Larmor frame, see S2E and Appendix C) by substituting appropriately for κ
- Must adjust element length consistently with composite replacement

E3

Case 2) The piecewise constant de-focusing transfer matrix $\mathbf{M}_x$ for $\kappa_x = -\kappa < 0$ can be resolved as:

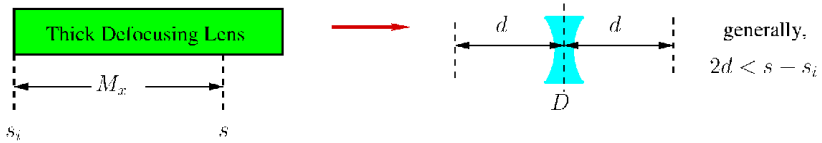

$$\mathbf{M_x}(s|s_i) = \begin{bmatrix} \text{Ch}(s) & \text{Sh}(s)/\sqrt{\kappa} \\ \sqrt{\kappa}\text{Sh}(s) & \text{Ch}(s) \end{bmatrix} = \begin{bmatrix} 1 & d(s) \\ 0 & 1 \end{bmatrix} \cdot \begin{bmatrix} 1 & 0 \\ 1/f(s) & 1 \end{bmatrix} \cdot \begin{bmatrix} 1 & d(s) \\ 0 & 1 \end{bmatrix} \equiv \mathbf{M}_{\text{drift}} \cdot \mathbf{M}_{\text{kick}} \cdot \mathbf{M}_{\text{drift}}$$

where

$\text{Ch}(s) = \cosh[\sqrt{\kappa}(s-s_i)]$ $\quad d(s) = \tanh[\sqrt{\kappa}(s-s_i)/2]/\sqrt{\kappa}$

$\text{Sh}(s) = \sinh[\sqrt{\kappa}(s-s_i)]$ $\quad 1/f(s) = \sqrt{\kappa}\text{Sh}(s)$

- Result is *exact* thin-lens equivalent defocusing element
- Can be applied together with thin lens focus replacement to more simply derive phase-advance formulas etc for AG focusing lattices
- Must adjust element length consistently with composite replacement

E4

Case 3) General element replacement with an equivalent thin lens

Consider a general transport matrix:

$$\mathbf{M} = \begin{bmatrix} M_{11} & M_{12} \\ M_{21} & M_{22} \end{bmatrix} \qquad \det\mathbf{M} = M_{11}M_{22} - M_{12}M_{21} = 1$$

- Always true for linear optics, see Sec S5

A transfer matrix of a drift of length d_1 followed by a thin lens of strength f, followed by a drift of length d_2 gives:

$$\mathbf{M}_{\text{drift2+thin+drift1}} = \begin{bmatrix} 1 & d_2 \\ 0 & 1 \end{bmatrix} \cdot \begin{bmatrix} 1 & 0 \\ -1/f & 1 \end{bmatrix} \cdot \begin{bmatrix} 1 & d_1 \\ 0 & 1 \end{bmatrix}$$

Setting $\mathbf{M} = \mathbf{M}_{\text{drift2+thin+drift1}}$

$$= \begin{bmatrix} 1 - d_2/f & d_1 + d_2 - d_1 d_2/f \\ -1/f & 1 - d_1/f \end{bmatrix}$$

$$\begin{aligned} d_1 &= (M_{22} - 1)/M_{21} \\ d_2 &= (M_{11} - 1)/M_{21} \\ -1/f &= M_{21} \end{aligned}$$

- M_{12} implicitly involved due to unit determinant constraint

Discussions of this, and similar results can be found in older optics books such as: Banford, *The Transport of Charged Particle Beams*, 1965.

E5

Comments:

- Shows that *any* linear optic (thick or thin) can be resolved into an equivalent thin lens kick + drifts
  - Use requires element effective length in drift + thin-lens-kick + drift to be adjusted consistently
  - Care must be taken to interpret lattice period with potentially different axial extent focusing elements correctly
- Orbits in thin-lens replacements may differ a little in max excursions etc, but this shows simple and rapid design estimates can be made using thin lens models if proper equivalences are employed
  - Analysis of thin lens + drifts can simplify interpretation and algebraic steps
- Construct applies to solenoidal focusing also if the orbit is analyzed in the Larmor frame where the decoupled orbit can be analyzed with Hill's equation, but it does *not* apply in the laboratory frame
  - Picewise contant (hard-edge) solenoid in lab frame can be resolved into a rotation + thin-lens kick structure though (see Appendix C)

E6

S3: Description of Applied Focusing Fields

S3A: Overview

Applied fields for focusing, bending, and acceleration enter the equations of motion via:

$\mathbf{E}^a$ = Applied Electric Field

$\mathbf{B}^a$ = Applied Magnetic Field

Generally, these fields are produced by sources (often static or slowly varying in time) located outside an aperture or so-called pipe radius $r = r_p$. For example, the electric and magnetic quadrupoles of S2:

Electric Quadrupole

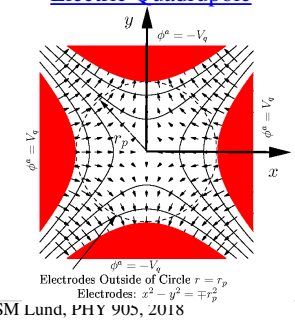

Hyperbolic material surfaces outside pipe radius

$r = r_p$

Magnetic Quadrupole

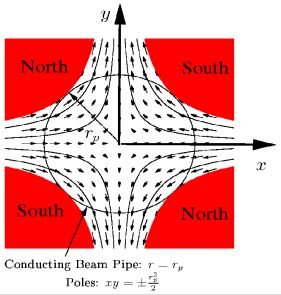

The fields of such classes of magnets obey the vacuum Maxwell Equations within the aperture:

$$\nabla \cdot \mathbf{E}^a = 0 \qquad \nabla \cdot \mathbf{B}^a = 0$$

$$\nabla \times \mathbf{E}^a = -\frac{\partial}{\partial t}\mathbf{B}^a \qquad \nabla \times \mathbf{B}^a = \frac{1}{c^2}\frac{\partial}{\partial t}\mathbf{E}^a$$

If the fields are static or sufficiently slowly varying (quasistatic) where the time derivative terms can be neglected, then the fields in the aperture will obey the static vacuum Maxwell equations:

$$\nabla \cdot \mathbf{E}^a = 0 \qquad \nabla \cdot \mathbf{B}^a = 0$$

$$\nabla \times \mathbf{E}^a = 0 \qquad \nabla \times \mathbf{B}^a = 0$$

In general, optical elements are tuned to limit the strength of nonlinear field terms so the beam experiences primarily linear applied fields.

- Linear fields allow better preservation of beam quality

Removal of *all* nonlinear fields cannot be accomplished

- 3D structure of the Maxwell equations precludes for finite geometry optics
- Even in finite geometries deviations from optimal structures and symmetry will result in nonlinear fields

As an example of this, when an ideal 2D iron magnet with infinite hyperbolic poles is truncated radially for finite 2D geometry, this leads to nonlinear focusing fields even in 2D:

- Truncation necessary along with confinement of return flux in yoke

Cross-Sections of Iron Quadrupole Magnets

Ideal (infinite geometry)

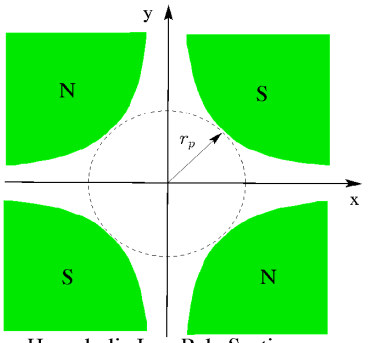

Hyperbolic Iron Pole Sections (infinite)

Practical (finite geometry)

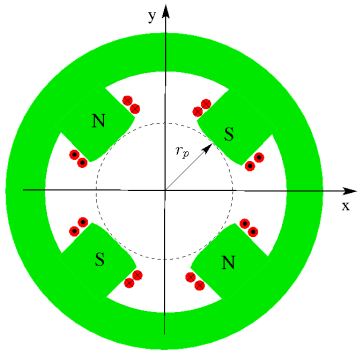

Shaped Iron Pole Sections (finite)

The design of optimized electric and magnetic optics for accelerators is a specialized topic with a vast literature. It is not be possible to cover this topic in this brief survey. In the remaining part of this section we will overview a limited subset of material on magnetic optics including:

- (see: S3B) Magnetic field expansions for focusing and bending
- (see: S3C) Hard edge equivalent models
- (see: S3D) 2D multipole models and nonlinear field scalings
- (see: S3E) Good field radius

Much of the material presented can be immediately applied to static Electric Optics since the vacuum Maxwell equations are the same for static Electric $\mathbf{E}^a$ and Magnetic $\mathbf{B}^a$ fields in vacuum.

S3B: Magnetic Field Expansions for Focusing and Bending

Forces from transverse $(B_z^a = 0)$ magnetic fields enter the transverse equations of motion (see: S1, S2) via:

Force: $\mathbf{F}_\perp^a \simeq q\beta_b c\hat{\mathbf{z}} \times \mathbf{B}_\perp^a$

Field: $\mathbf{B}_\perp^a = \hat{\mathbf{x}} B_x^a + \hat{\mathbf{y}} B_y^a$

Combined these give:

$$\boxed{\begin{aligned} F_x^a &\simeq -q\beta_b c B_y^a \\ F_y^a &\simeq \; q\beta_b c B_x^a \end{aligned}}$$

Field components entering these expressions can be expanded about $\mathbf{x}_\perp = 0$

- Element center and design orbit taken to be at $\mathbf{x}_\perp = 0$

$$B_x^a = \overset{1}{B_x^a}(0) + \overset{2}{\frac{\partial B_x^a}{\partial y}}(0)y + \overset{3}{\frac{\partial B_x^a}{\partial x}}(0)x$$

Nonlinear Focus

$$+\frac{1}{2}\frac{\partial^2 B_x^a}{\partial x^2}(0)x^2 + \frac{\partial^2 B_x^a}{\partial x \partial y}(0)xy + \frac{1}{2}\frac{\partial B_x^a}{\partial y^2}(0)y^2 + \cdots$$

$$B_y^a = \overset{1}{B_y^a}(0) + \overset{2}{\frac{\partial B_y^a}{\partial x}}(0)x + \overset{3}{\frac{\partial B_y^a}{\partial y}}(0)y$$

Nonlinear Focus

$$+\frac{1}{2}\frac{\partial^2 B_y^a}{\partial x^2}(0)x^2 + \frac{\partial^2 B_y^a}{\partial x \partial y}(0)xy + \frac{1}{2}\frac{\partial B_y^a}{\partial y^2}(0)y^2 + \cdots$$

Terms:
1: Dipole Bend
2: Normal Quad Focus
3: Skew Quad Focus

Sources of undesired nonlinear applied field components include:

- Intrinsic finite 3D geometry and the structure of the Maxwell equations
- Systematic errors or sub-optimal geometry associated with practical trade-offs in fabricating the optic
- Random construction errors in individual optical elements
- Alignment errors of magnets in the lattice giving field projections in unwanted directions
- Excitation errors effecting the field strength
  - Currents in coils not correct and/or unbalanced

More advanced treatments exploit less simple power-series expansions to express symmetries more clearly:

- Maxwell equations constrain structure of solutions
  - Expansion coefficients are NOT all independent
- Forms appropriate for bent coordinate systems in dipole bends can become complicated

S3C: Hard Edge Equivalent Models

Real 3D magnets can often be modeled with sufficient accuracy by 2D hard-edge "equivalent" magnets that give the same approximate focusing impulse to the particle as the full 3D magnet

- Objective is to provide same approximate applied focusing "kick" to particles with different focusing gradient functions $G(s)$

See Figure Next Slide

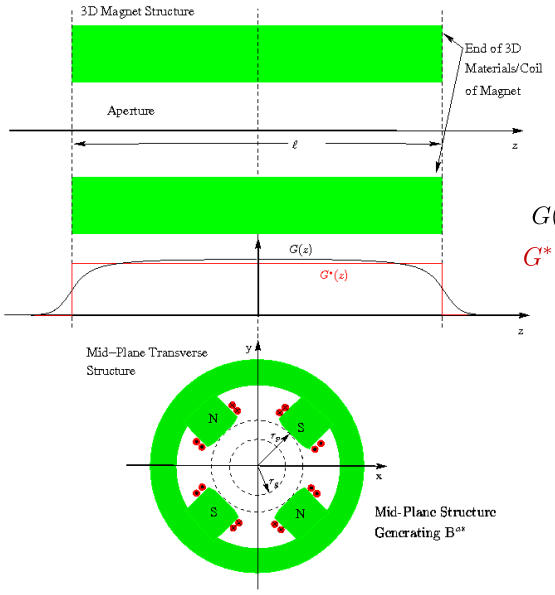

$G(z)$ = 3D Field Gradient

$G^*(z)$ = Hard-Edge Equivalent Field Gradient

Many prescriptions exist for calculating the effective axial length and strength of hard-edge equivalent models

- See Review: Lund and Bukh, PRSTAB 7 204801 (2004), Appendix C

Here we overview a simple equivalence method that has been shown to work well:

For a relatively long, but finite axial length magnet with 3D gradient function:

$$G(z) \equiv \left.\frac{\partial B_x^a}{\partial y}\right|_{x=y=0}$$

Take hard-edge equivalent parameters:

- Take z = 0 at the axial magnet mid-plane

Gradient: $G^* \equiv G(z=0)$

Axial Length: $\ell \equiv \dfrac{1}{G(z=0)} \displaystyle\int_{-\infty}^{\infty} dz\, G(z)$

- More advanced equivalences can be made based more on particle optics
  - Disadvantage of such methods is "equivalence" changes with particle energy and must be revisited as optics are tuned

S3D: 2D Transverse Multipole Magnetic Fields

In many cases, it is sufficient to characterize the field errors in 2D hard-edge equivalent as:

$$\overline{B_x}(x,y) = \frac{1}{\ell}\int_{-\infty}^{\infty} dz\; B_x^a(x,y,z)$$
$$\overline{B_y}(x,y) = \frac{1}{\ell}\int_{-\infty}^{\infty} dz\; B_y^a(x,y,z)$$

2D Effective Fields — 3D Fields

Operating on the vacuum Maxwell equations with: $\displaystyle\int_{-\infty}^{\infty} \frac{dz}{\ell}\cdots$

yields the (exact) 2D Transverse Maxwell equations :

$$\frac{\partial \overline{B_x}(x,y)}{\partial y} = \frac{\partial \overline{B_y}(x,y)}{\partial x} \quad \Leftarrow \text{ From } \nabla\times\mathbf{B}=0$$
$$\frac{\partial \overline{B_x}(x,y)}{\partial x} = -\frac{\partial \overline{B_y}(x,y)}{\partial y} \quad \Leftarrow \text{ From } \nabla\cdot\mathbf{B}=0$$

These equations are recognized as the Cauchy-Riemann conditions for a complex field variable:

$$\underline{B}^* \equiv \overline{B_x} - i\overline{B_y} \qquad i \equiv \sqrt{-1}$$

to be an analytical function of the complex variable:

$$\underline{z} \equiv x + iy \qquad i \equiv \sqrt{-1}$$

Notation: Underlines denote complex variables where confusion may arise

Cauchy-Riemann Conditions	2D Magnetic Field
$\underline{F} = u(x,y) + iv(x,y)$	$u = \overline{B_x} \quad v = -\overline{B_y}$
$\dfrac{\partial u}{\partial x} = \dfrac{\partial v}{\partial y}$	$\longrightarrow \quad \dfrac{\partial \overline{B_x}(x,y)}{\partial x} = -\dfrac{\partial \overline{B_y}(x,y)}{\partial y}$
$\dfrac{\partial u}{\partial y} = -\dfrac{\partial v}{\partial x}$	$\longrightarrow \quad \dfrac{\partial \overline{B_x}(x,y)}{\partial y} = \dfrac{\partial \overline{B_y}(x,y)}{\partial x}$
$\underline{F} = u + iv$ analytic func of $\underline{z} = x + iy$	$\underline{F} = \overline{B_x} - i\overline{B_y}$ analytic func of $\underline{z} = x + iy$

Note the complex field which is an analytic function of $\underline{z} = x + iy$ is $\underline{B}^* = \overline{B_x} - i\overline{B_y}$ NOT $\underline{B} = \overline{B_x} + i\overline{B_y}$. This is *not* a typo and is necessary for $\underline{B}^*$ to satisfy the Cauchy-Riemann conditions.

- See problem sets for illustration

It follows that $\underline{B}^*(\underline{z})$ can be analyzed using the full power of the highly developed theory of analytical functions of a complex variable.

Expand $\underline{B}^*(\underline{z})$ as a Laurent Series within the vacuum aperture as:

$$\underline{B}^*(\underline{z}) = \overline{B_x}(x,y) - i\overline{B_y}(x,y) = \sum_{n=1}^{\infty} \underline{b}_n \underline{z}^{n-1}$$

$$\underline{b}_n = \text{const (complex)}$$

$$n = \text{Multipole Index}$$

The $\underline{b}_n$ are called "multipole coefficients" and give the structure of the field. The multipole coefficients can be resolved into real and imaginary parts as:

$$\underline{b}_n = \mathcal{A}_n - i\mathcal{B}_n$$

$$\mathcal{B}_n \Longrightarrow \text{"Normal" Multipoles}$$

$$\mathcal{A}_n \Longrightarrow \text{"Skew" Multipoles}$$

Some algebra identifies the polynomial symmetries of low-order terms as:

Cartesian projections: $\overline{B_x} - i\overline{B_y} = (\mathcal{A}_n - i\mathcal{B}_n)(x+iy)^{n-1}$

Index	Name	Normal ($\mathcal{A}_n = 0$)		Skew ($\mathcal{B}_n = 0$)	
n		$\overline{B_x}/\mathcal{B}_n$	$\overline{B_y}/\mathcal{B}_n$	$\overline{B_x}/\mathcal{A}_n$	$\overline{B_y}/\mathcal{A}_n$
1	Dipole	0	1	1	
2	Quadrupole	y	x	x	$-y$
3	Sextupole	$2xy$	x^2-y^2	x^2-y^2	$-2xy$
4	Octupole	$3x^2y-y^3$	x^3-3xy^2	x^3-3xy^2	$-3x^2y+y^3$
5	Decapole	$4x^3y-4xy^3$	$x^4-6x^2y^2+y^4$	$x^4-6x^2y^2+y^4$	$-4x^3y+4xy^3$

Comments:

- Reason for pole names most apparent from polar representation (see following pages) and sketches of the magnetic pole structure
- Caution: In so-called "US notation", poles are labeled with index *n* -> *n* -1
  - Arbitrary in 2D but US choice *not* good notation in 3D generalizations

Comments continued:

- Normal and Skew symmetries can be taken as a symmetry *definition.* But this choice makes sense for *n* = 2 quadrupole focusing terms:

$$\overline{F_x^a} = -q\beta_b c\overline{B_y} \quad = -q\beta_b c(\mathcal{B}_2 x - \mathcal{A}_2 y)$$

$$\overline{F_y^a} = \quad q\beta_b c\overline{B_x} \quad = \quad q\beta_b c(\mathcal{B}_2 y + \mathcal{A}_2 x)$$

In equations of motion:

Normal	$\Rightarrow$	$\mathcal{B}_2$:	x-eqn, x-focus	y-eqn, y-defocus
Skew	$\Rightarrow$	$\mathcal{A}_2$:	x-eqn, y-defocus	y-eqn, x-defocus

Magnetic Pole Symmetries (normal orientation):

Dipole (n=1) Quadrupole (n=2) Sextupole (n=3)

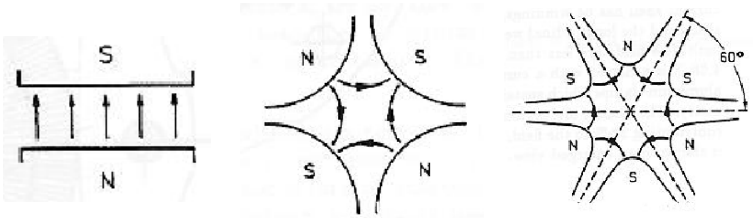

- Actively rotate normal field structures clockwise through an angle of $\pi/(2n)$ for skew field component symmetries

Multipole scale/units

Frequently, in the multipole expansion:

$$\underline{B}^*(\underline{z}) = \overline{B_x}(x,y) - i\overline{B_y}(x,y) = \sum_{n=1}^{\infty} \underline{b}_n \underline{z}^{n-1}$$

the multipole coefficients $\underline{b}_n$ are rescaled as

$$\underline{b}_n \rightarrow \underline{b}_n r_p^{n-1} \qquad r_p = \text{Aperture "Pipe" Radius}$$

Closest radius of approach of magnetic sources and/or aperture materials

so that the expansions becomes

$$\underline{B}^*(\underline{z}) = \overline{B_x}(x,y) - i\overline{B_y}(x,y) = \sum_{n=1}^{\infty} \underline{b}_n \left(\frac{\underline{z}}{r_p}\right)^{n-1}$$

Advantages of alternative notaiton:

- Multipoles $\underline{b}_n$ given directly in field units regardless of index *n*
- Scaling of field amplitudes with radius within the magnet bore becomes clear

Scaling of Fields produced by multipole term:

Higher order multipole coefficients (larger n values) leading to nonlinear focusing forces decrease rapidly within the aperture. To see this use a polar representation for $\underline{z}$, $\underline{b}_n$

$$\underline{z} = x + iy = re^{i\theta} \qquad r = \sqrt{x^2 + y^2}$$
$$\theta = \arctan[y, x]$$
$$\underline{b}_n = |\underline{b}_n| e^{i\psi_n} \qquad \psi_n = \text{Real Const}$$

Thus, the nth order multipole terms scale as

$$\underline{b}_n \left(\frac{\underline{z}}{r_p}\right)^{n-1} = |\underline{b}_n| \left(\frac{r}{r_p}\right)^{n-1} e^{i[(n-1)\theta + \psi_n]}$$

- Unless the coefficient $|\underline{b}_n|$ is very large, high order terms in n will become small rapidly as r_p decreases
- Better field quality can be obtained for a given magnet design by simply making the clear bore r_p larger, or alternatively using smaller bundles (more tight focus) of particles
  - Larger bore machines/magnets cost more. So designs become trade-off between cost and performance.
  - Stronger focusing to keep beam from aperture can be unstable (see: S5)

S3E: Good Field Radius

Often a magnet design will have a so-called "good-field" radius $r = r_g$ that the maximum field errors are specified on.

- In superior designs the good field radius can be around ~70% or more of the clear bore aperture to the beginning of material structures of the magnet.
- Beam particles should evolve with radial excursions with $r < r_g$

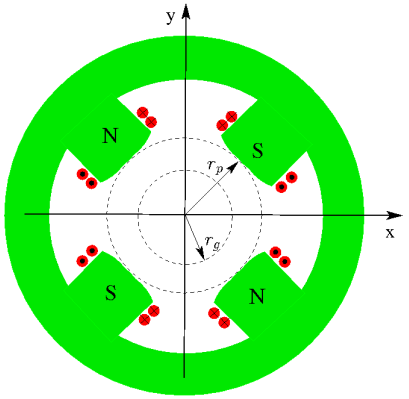

r_p = Clear Bore Radius
$\sim$ Pole Radius Typical

r_g = Good Field Radius
$\sim$ 70% r_p Typical

Comments:

- Particle orbits are designed to remain within radius r_g
- Field error statements are readily generalized to 3D since:

$$\nabla \cdot \mathbf{B}^a = 0$$
$$\nabla \times \mathbf{B}^a = 0 \quad \Longrightarrow \quad \nabla^2 \mathbf{B}^a = 0$$

and therefore each component of $\mathbf{B}^a$ satisfies a Laplace equation within the vacuum aperture. Therefore, field errors decrease when moving more deeply within a source-free region.

S3F: Example Permanent Magnet Assemblies

A few examples of practical permanent magnet assemblies with field contours are provided to illustrate error field structures in practical devices

8 Rectangular Block Dipole

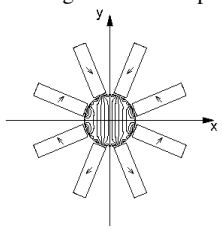

8 Square Block Quadrupole

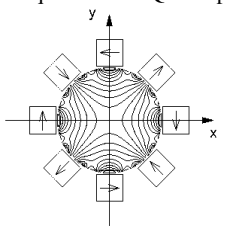

12 Rectangular Block Sextupole

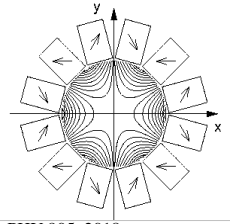

8 Rectangular Block Quadrupole

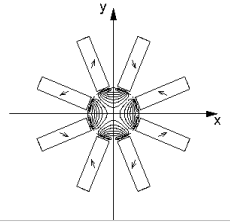

For more info on permanent magnet design see: Lund and Halbach, Fusion Engineering Design, **32-33**, 401-415 (1996)

S4: Transverse Particle Equations of Motion with Nonlinear Applied Fields — S4A: Overview

In S1 we showed that the particle equations of motion can be expressed as:

$$\mathbf{x}_\perp'' + \frac{(\gamma_b\beta_b)'}{(\gamma_b\beta_b)}\mathbf{x}_\perp' = \frac{q}{m\gamma_b\beta_b^2c^2}\mathbf{E}_\perp^a + \frac{q}{m\gamma_b\beta_bc}\hat{\mathbf{z}}\times\mathbf{B}_\perp^a + \frac{qB_z^a}{m\gamma_b\beta_bc}\mathbf{x}_\perp'\times\hat{\mathbf{z}} - \frac{q}{\gamma_b^3\beta_b^2c^2}\frac{\partial}{\partial\mathbf{x}_\perp}\phi$$

When momentum spread is neglected and results are interpreted in a Cartesian coordinate system (no bends). In S2, we showed that these equations can be further reduced when the applied focusing fields are linear to:

$$x'' + \frac{(\gamma_b\beta_b)'}{(\gamma_b\beta_b)}x' + \kappa_x(s)x = -\frac{q}{m\gamma_b^3\beta_b^2c^2}\frac{\partial}{\partial x}\phi$$

$$y'' + \frac{(\gamma_b\beta_b)'}{(\gamma_b\beta_b)}y' + \kappa_y(s)y = -\frac{q}{m\gamma_b^3\beta_b^2c^2}\frac{\partial}{\partial y}\phi$$

where $\kappa_x(s) = x$-focusing function of lattice

$\kappa_y(s) = y$-focusing function of lattice

describe the linear applied focusing forces and the equations are implicitly analyzed in the rotating Larmor frame when $B_z^a \neq 0$.

Lattice designs attempt to minimize nonlinear applied fields. However, the 3D Maxwell equations show that there will *always* be some finite nonlinear applied fields for an applied focusing element with finite extent. Applied field nonlinearities also result from:

- Design idealizations
- Fabrication and material errors

The largest source of nonlinear terms will depend on the case analyzed.

Nonlinear applied fields must be added back in the idealized model when it is appropriate to analyze their effects

- Common problem to address when carrying out large-scale numerical simulations to design/analyze systems

There are two basic approaches to carry this out:

Approach 1: Explicit 3D Formulation

Approach 2: Perturbations About Linear Applied Field Model

We will now discuss each of these in turn

S4B: Approach 1: Explicit 3D Formulation

This is the simplest. Just employ the full 3D equations of motion expressed in terms of the applied field components $\mathbf{E}^a$, $\mathbf{B}^a$ and avoid using the focusing functions κ_x, κ_y

Comments:

- Most easy to apply in computer simulations where many effects are simultaneously included
  - Simplifies comparison to experiments when many details matter for high level agreement
- Simplifies simultaneous inclusion of transverse and longitudinal effects
  - Accelerating field E_z^a can be included to calculate changes in β_b, γ_b
  - Transverse and longitudinal dynamics cannot be fully decoupled in high level modeling – especially try when acceleration is strong in systems like injectors
- Can be applied with time based equations of motion (see: S1)
  - Helps avoid unit confusion and continuously adjusting complicated equations of motion to identify the axial coordinate s appropriately

S4C: Approach 2: Perturbations About Linear Applied Field Model

Exploit the linearity of the Maxwell equations to take:

$$\mathbf{E}_\perp^a = \mathbf{E}_\perp^a|_L + \delta\mathbf{E}_\perp^a$$

$$\mathbf{B}^a = \mathbf{B}^a|_L + \delta\mathbf{B}^a$$

where

$\mathbf{E}_\perp^a|_L$, $\mathbf{B}^a|_L$ are the linear field components incorporated in κ_x, κ_y

to express the equations of motion as:

$$x'' + \frac{(\gamma_b\beta_b)'}{(\gamma_b\beta_b)}x' + \kappa_x x = \frac{q}{m\gamma_b\beta_b^2c^2}\delta E_x^a - \frac{q}{m\gamma_b\beta_bc}\delta B_y^a + \frac{q}{m\gamma_b\beta_bc}\delta B_z^a y' - \frac{q}{m\gamma_b^3\beta_b^2c^2}\frac{\partial\phi}{\partial x}$$

$$y'' + \frac{(\gamma_b\beta_b)'}{(\gamma_b\beta_b)}y' + \kappa_y y = \frac{q}{m\gamma_b\beta_b^2c^2}\delta E_y^a + \frac{q}{m\gamma_b\beta_bc}\delta B_x^a - \frac{q}{m\gamma_b\beta_bc}\delta B_z^a x' - \frac{q}{m\gamma_b^3\beta_b^2c^2}\frac{\partial\phi}{\partial y}$$

This formulation can be most useful to understand the effect of deviations from the usual linear model where intuition is developed

Comments:

- Best suited to non-solenoidal focusing
  - Simplified Larmor frame analysis for solenoidal focusing is only valid for axisymmetric potentials $\phi = \phi(r)$ which may not hold in the presence of non-ideal perturbations.
  - Applied field perturbations $\delta\mathbf{E}^a_\perp,\ \delta\mathbf{B}^a$ would also need to be projected into the Larmor frame
- Applied field perturbations $\delta\mathbf{E}^a_\perp,\ \delta\mathbf{B}^a$ will not necessarily satisfy the 3D Maxwell Equations by themselves
  - Follows because the linear field components $\mathbf{E}^a_\perp|_L,\ \mathbf{B}^a|_L$ will not, in general, satisfy the 3D Maxwell equations by themselves

Corrections and suggestions for improvements welcome!

These notes will be corrected and expanded for reference and for use in future editions of US Particle Accelerator School (USPAS) and Michigan State University (MSU) courses. Contact:

Prof. Steven M. Lund
Facility for Rare Isotope Beams
Michigan State University
640 South Shaw Lane
East Lansing, MI 48824

lund@frib.msu.edu
(517) 908 – 7291 office
(510) 459 - 4045 mobile

Please provide corrections with respect to the present archived version at:

https://people.nscl.msu.edu/~lund/msu/phy905_2018